



**UNIVERSITY OF ROME “LA SAPIENZA”
NANOTECHNOLOGIES ENGINEERING**

MICROPARTICLES CHARACTERIZATION

PROF. MARCO STOLLER

DEPARTMENT OF CHEMICAL MATERIALS ENVIRONMENTAL ENGINEERING

2ND FLOOR – ROOM 205

TEL: +390644585580

MARCO.STOLLER@UNIROMA1.IT

Main issues to be monitored

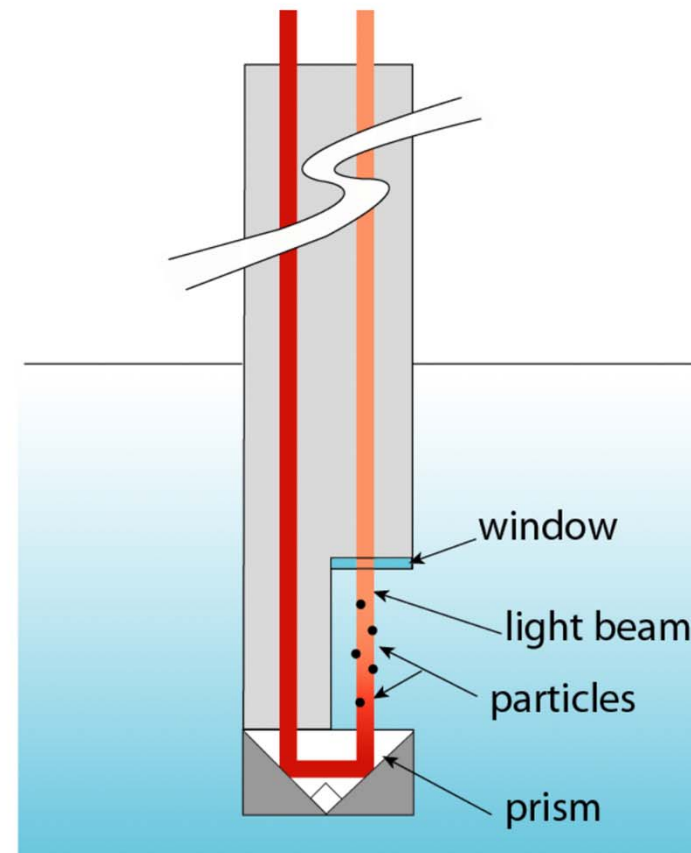
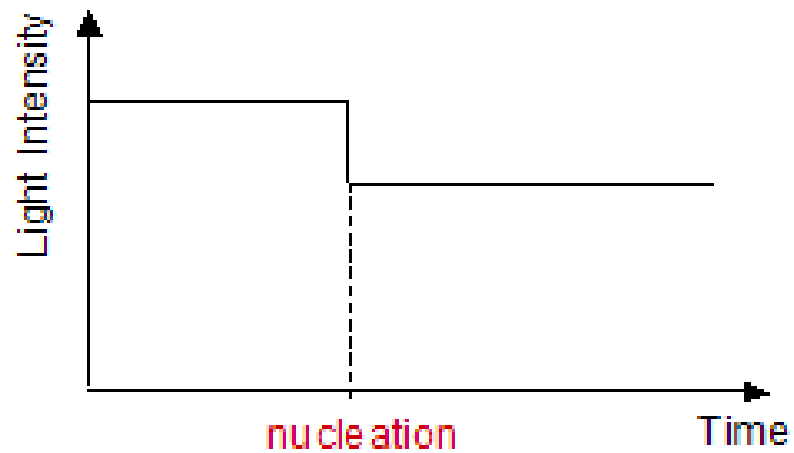
- The nucleation point in batch operation
- The crystal habit
- The crystal size distribution and/or the magma density of fines

Sensors to measure the nucleation point

- In the lab experiments, by using vessels made by glass, the sensor can be the human eye, but it cannot be the case for industrial apparatuses.
- In-situ instruments are based on the physical change in the medium, as:
 - Light transmittance
 - Light diffusion
 - Others: Ultrasound transmission, Electrical conductivity, etc.

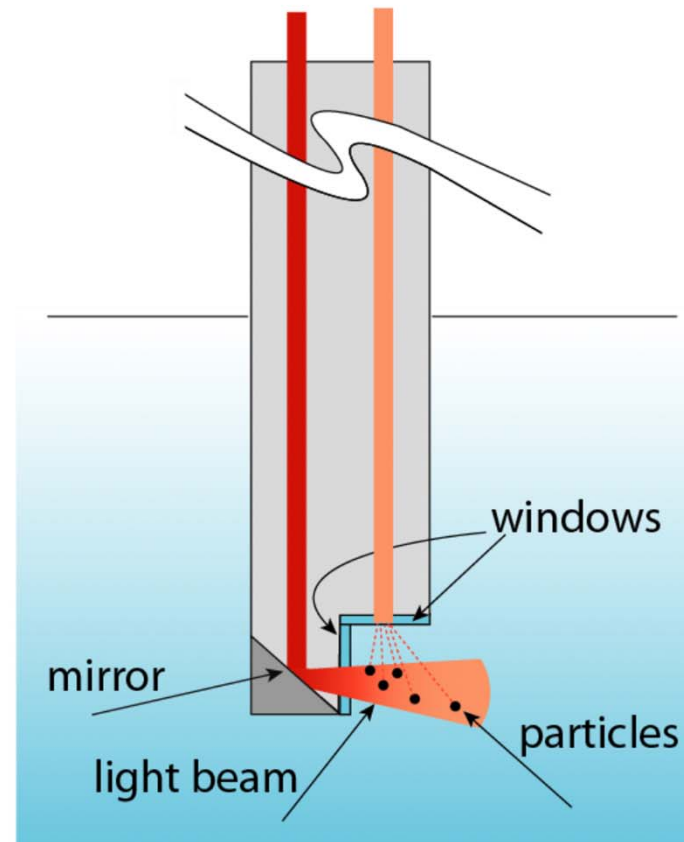
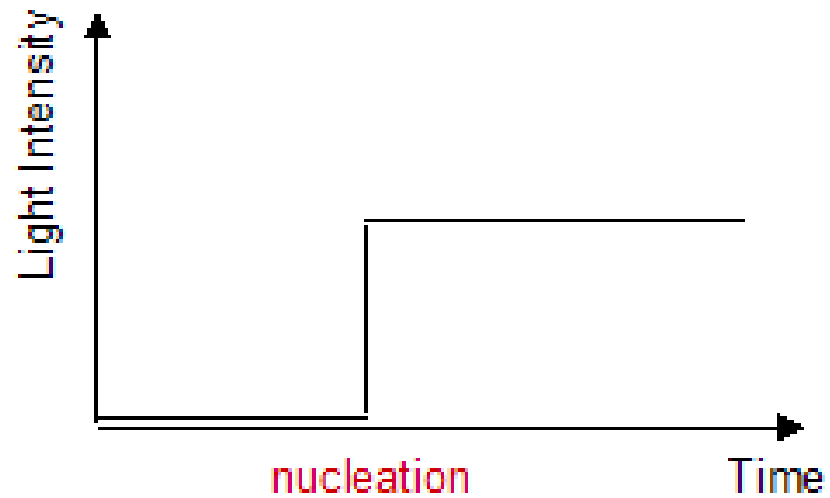
Turbidimetric probe

It measures the transmitted light intensity



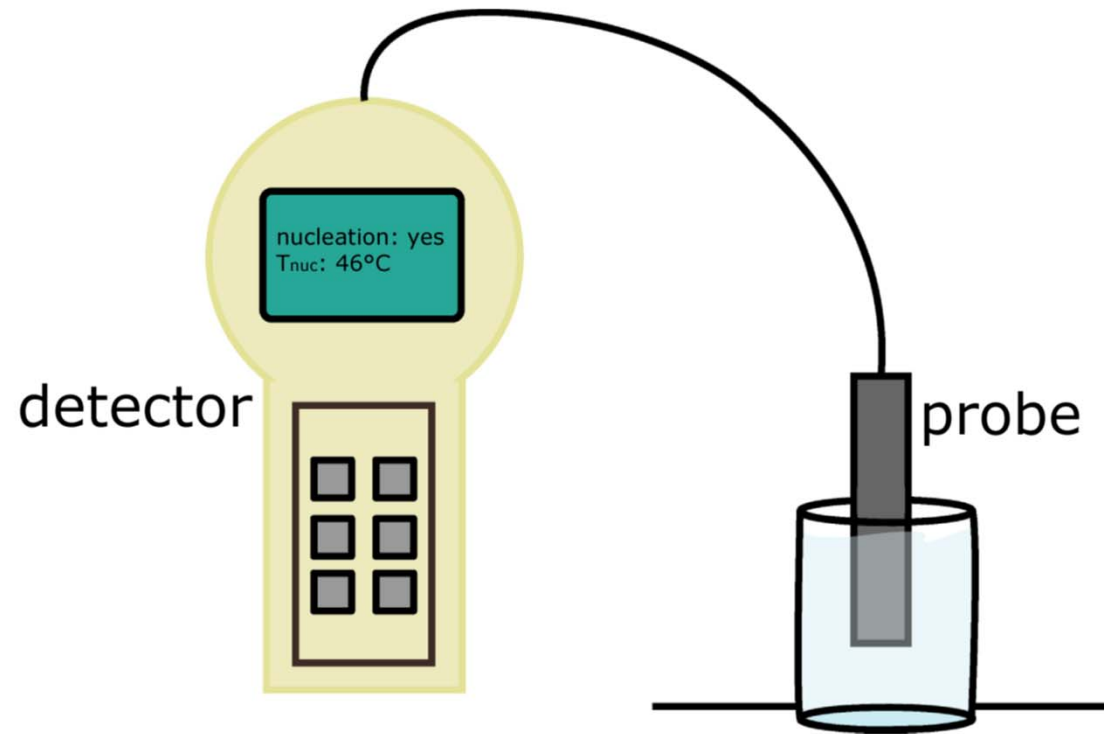
Nephelometric probe

It measures the light diffusion intensity

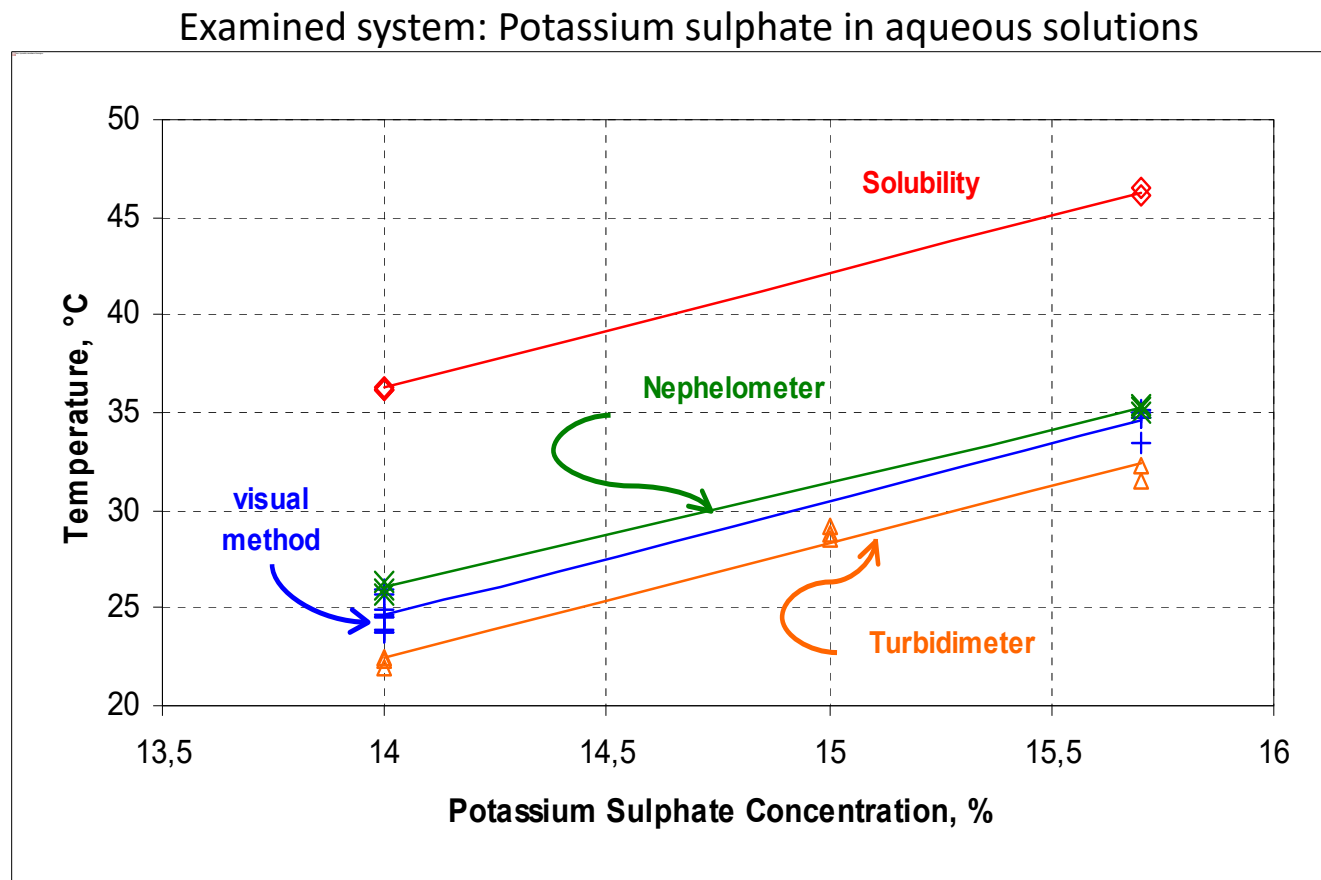


The overall instrument

The probe measures light intensity and temperature



Comparison between Turbidimetric and Nephelometric methods



Comparison between Turbid metric and Nephelometric methods

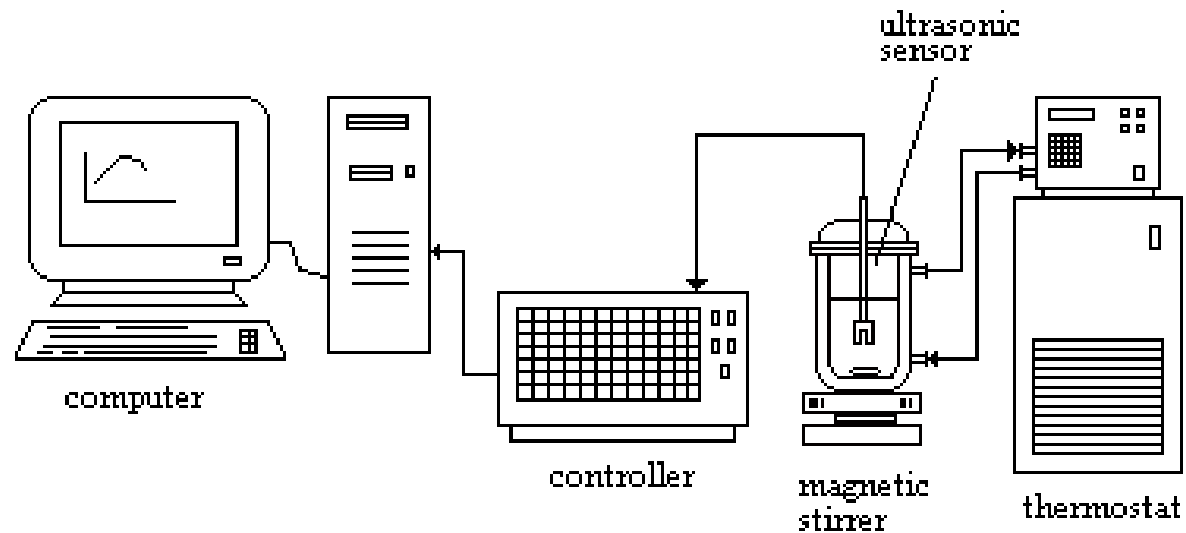
Examined system: Dextrose in aq. solutions

$$\Delta T = T_{\text{eye}} - T_{\text{probe}}$$

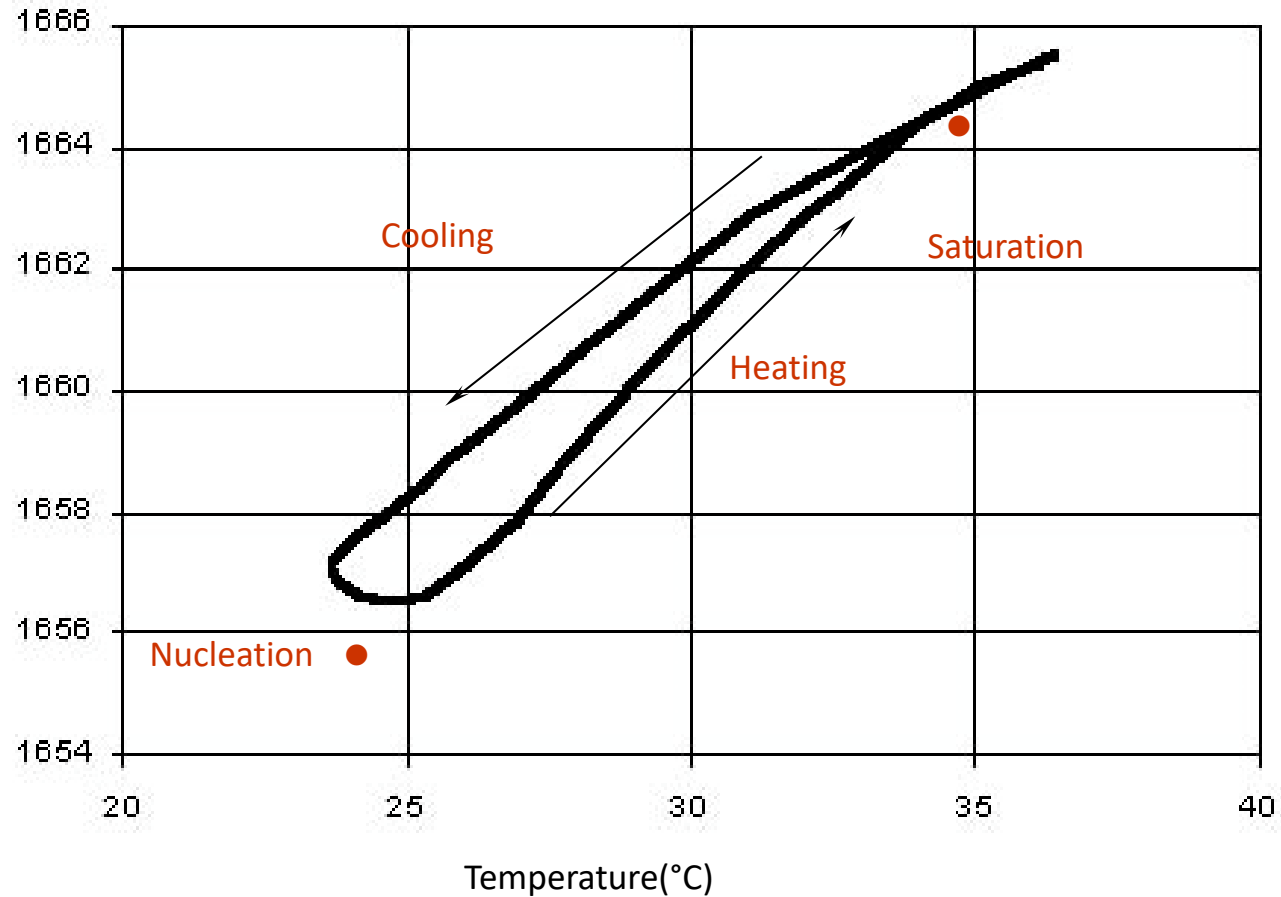
DX concentr. g/g solution	Nephelometry ΔT, °C	Turbidimetry ΔT, °C
0.665	0.65	2.60
0.568	0.03	1.70

ULTRASOUND METHOD

Overall experimental set-up



METASTABLE ZONE LIMITS



Ultrasonic method cannot be used for all the systems

NUCLEATION POINT DETECTION: CONCLUSIONS

- The methods based on the measurements of the light intensity are the easiest ones.
- Nephelometry is the better method.
- Ultrasonic sound method works, but cannot be applied to all the systems.

OUTLINE - SIZE DISTRIBUTION CHARACTERISTICS

- **CSD Measurements**
 - Off-line sensors: Sieving, Image analyser, Forward laser-light diffraction
 - In-situ on-line sensors: Back-scattering, image analyser
 - On-line sensors: Ultrasonic attenuation
- **Fines content**
 - On-line and off-line sensors based on a turbidimetric cell

Why to measure CSDs ?

- To check the characteristics of the final crystal product.
 - The measurement procedure should be set up in the selling contract.
- To monitor and control the crystallization processes.
 - CSD deviations are of interest.
- To investigate crystal growth kinetics.
 - The kind of measurement has to be consistent with the kinetic objectives.

SIEVING ANALYSIS

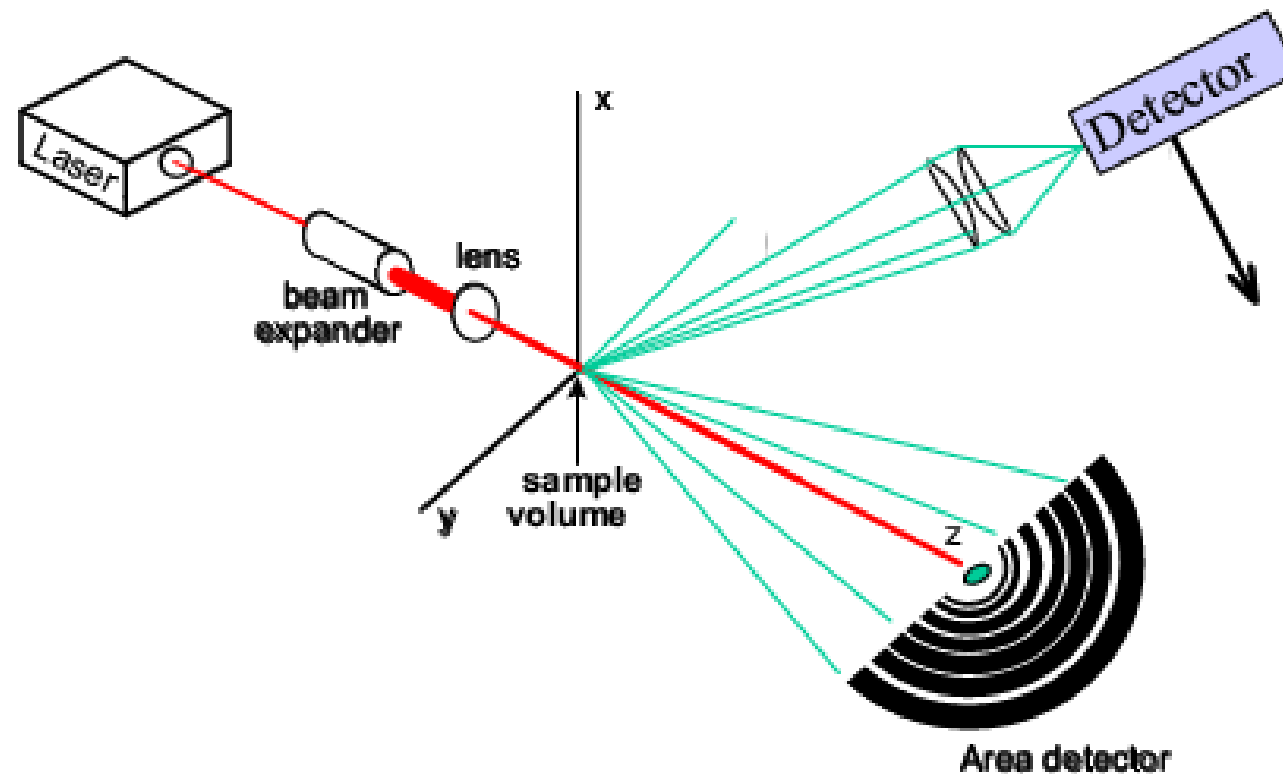
- The oldest and still the most used technique in the industry
- It determines the size distribution with respect to the second crystal dimension



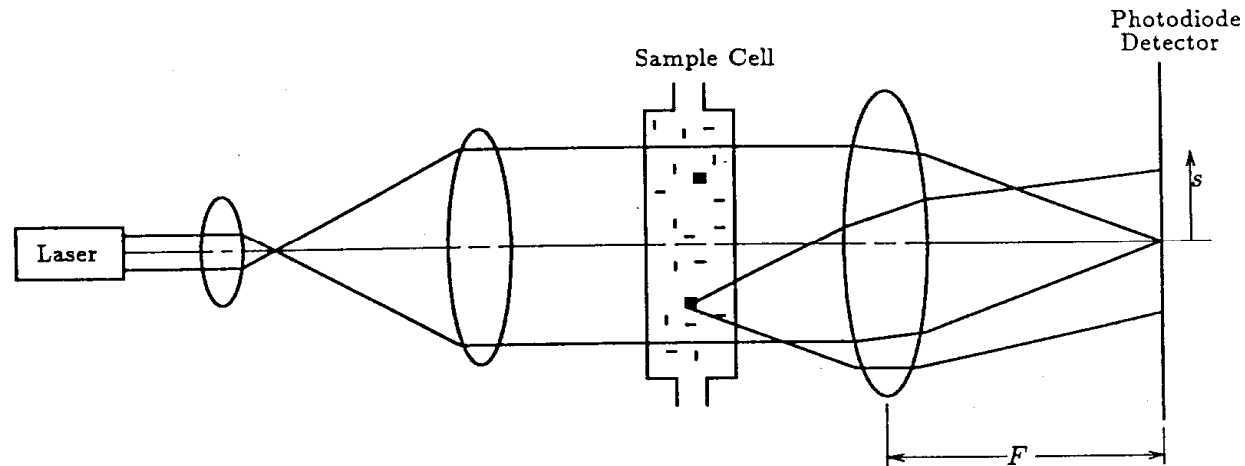
- When the crystals are prone to sticking, **wet sieving** must be adopted
- The **minimum measurable size** is equal to **20-30 microns** by using an **upward gas stream**

FORWARD LIGHT SCATTERING

The diffraction of a parallel beam due to crystal suspension gives rise to a composite scatter pattern.



Principles of FLS



- An intensity pattern may be recorded as a function of the **scatter angle**, with an inner radius s_i .
- The **energy scattered** by the particles of radius L , $e'(L, s_i)$, is given by the **Fraunhofer equation**.

Crystal size distribution evaluation

$$\begin{pmatrix} e_t(s_1) \\ \cdot \\ \cdot \\ e_t(s_n) \end{pmatrix} = \begin{pmatrix} w_1 e'(L_1, s_1) & \cdot & \cdot & w_p e'(L_p, s_1) \\ \cdot & \cdot & \cdot & \cdot \\ \cdot & \cdot & \cdot & \cdot \\ w_1 e'(L_1, s_n) & \cdot & \cdot & w_p e'(L_1, s_n) \end{pmatrix} \cdot \begin{pmatrix} m(L_1) \\ \cdot \\ \cdot \\ m(L_p) \end{pmatrix}$$

where the vectors e_t and m are the **measured light energy** and the **unknown size distribution**

- A deconvolution technique must be used to solve the unknown mass density distribution

Limitation of the FLS technique

- The Fraunhofer approximation predicts the energy scattered by a spherical particle of radius L , that is the approach is not appropriate for quite elongated particles.
- A correction proposed by Brown and Felton may be useful to set up a correspondence between the measured size and that one of the real particle.

Comparison between CSDs from Image analysis and FLS techniques

- Examined case: Dextrose monohydrate crystals

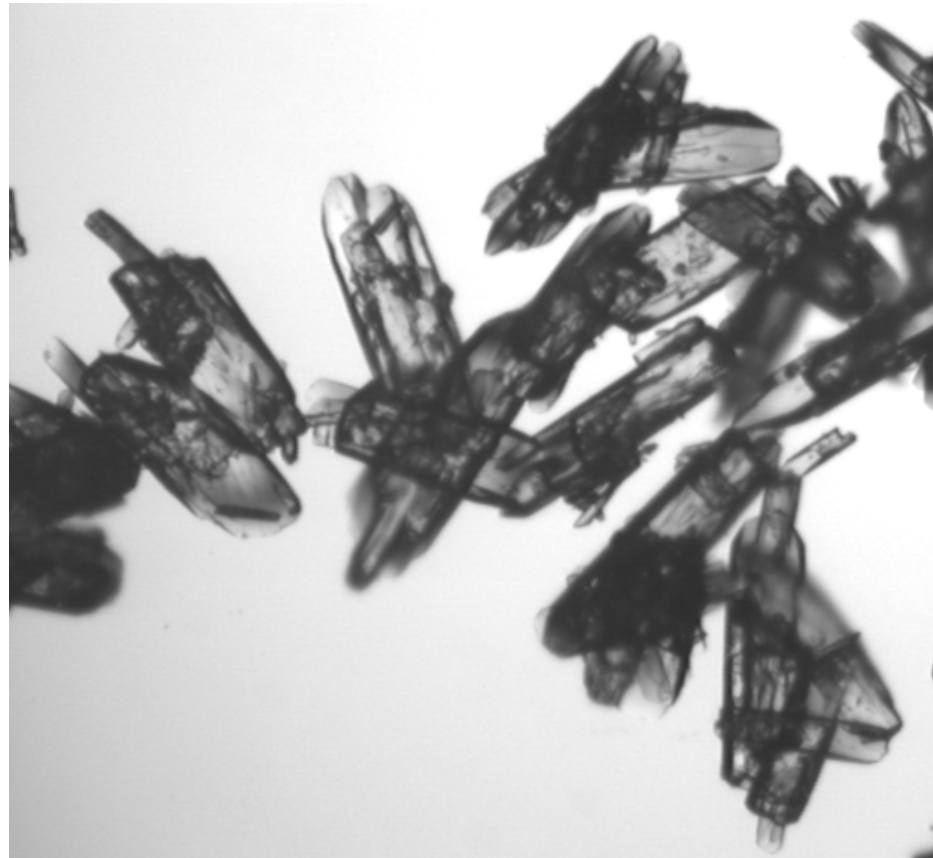
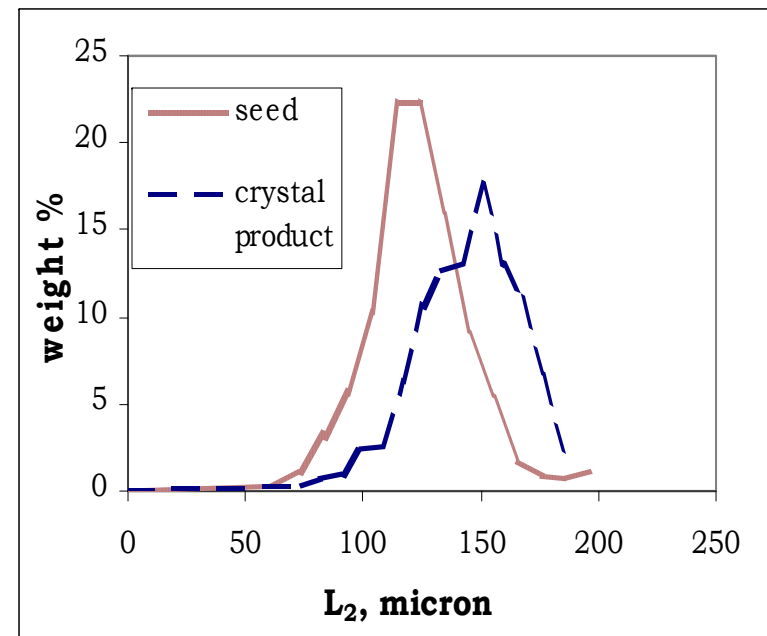
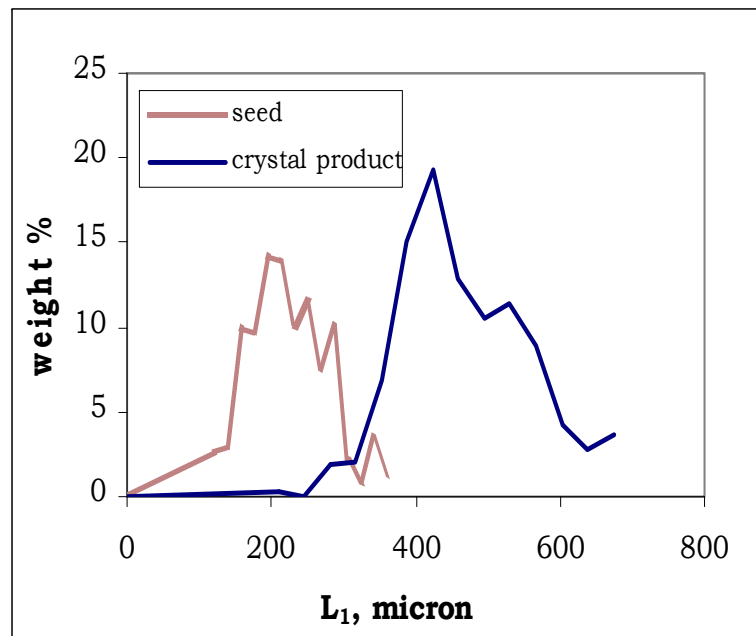


Image Analysis of DX crystals from a batch crystallization process

Examined crystals: Seeds and Crystal Product

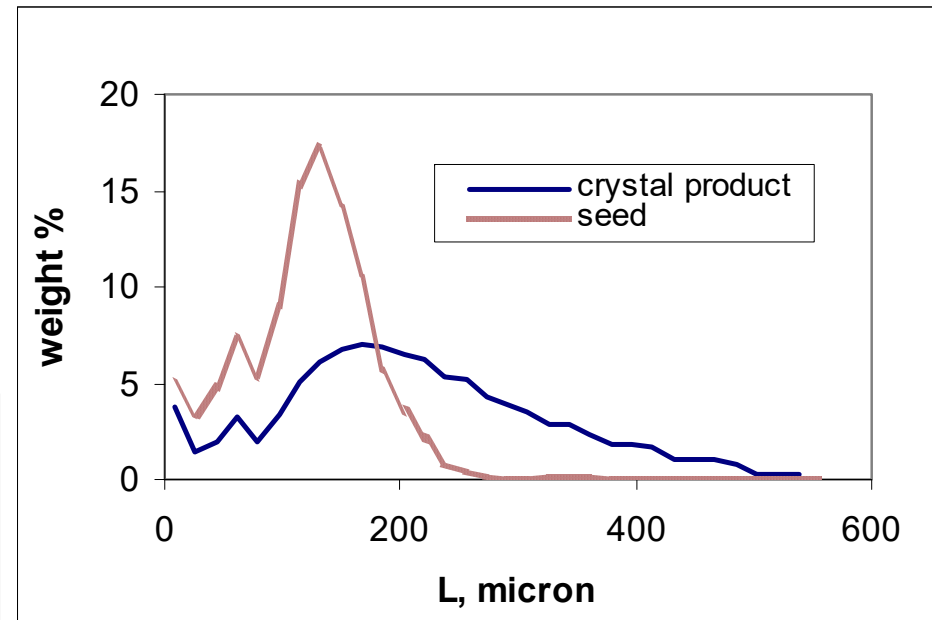
L_1 first dimension, L_2 second dimension; $L_1/L_2 \cong 3$



FLS results and Comparison with the image analysis technique

Comparison
between the two techniques

	Image Analysis average values		FLS av values
	$L_1, \mu\text{m}$	$L_2, \mu\text{m}$	$L, \mu\text{m}$
Seed	208	117	129
Prod.	436	137	201



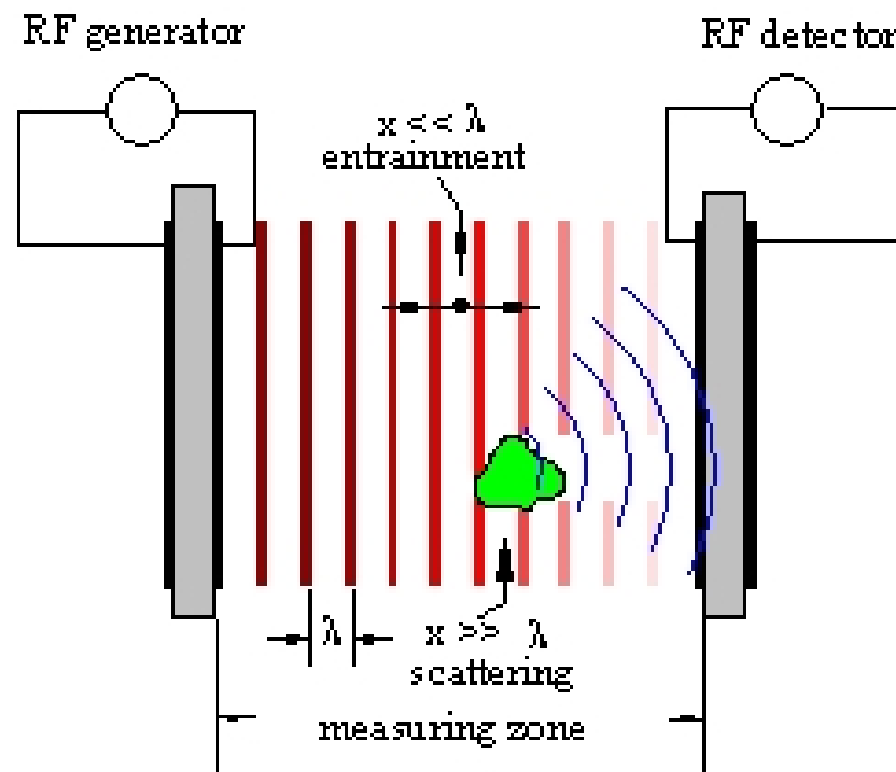
FLS
Results

FLS - Conclusions

- High resolution and good reproducibility.
- A projected area based volume distribution.
- Wide measuring range: $<1\mu\text{m} \rightarrow 6000\mu\text{m}$
- On line application requires a severe sample dilution ($< 1\%$).
- A shape different from the spherical one needs additional correction.

Ultrasonic attenuation

An electrical high frequency generator is connected to a piezoelectric ultrasonic transducer. The ultrasonic pulse interacts with the suspended particles.



Prediction of CSD by ultrasonic attenuation

The attenuation of the ultrasonic waves of frequency f_i for a projection area concentration c_{PF} is given by:

$$\alpha(f_i, L) = \frac{1}{\Delta S \cdot c_{PF}} \ln(I_0/I)_{f_i}$$

for the size L

and

$$a_T(f_i) = \int_0^{\infty} \alpha(f_i, L) \cdot f(L) dL$$

for all sizes

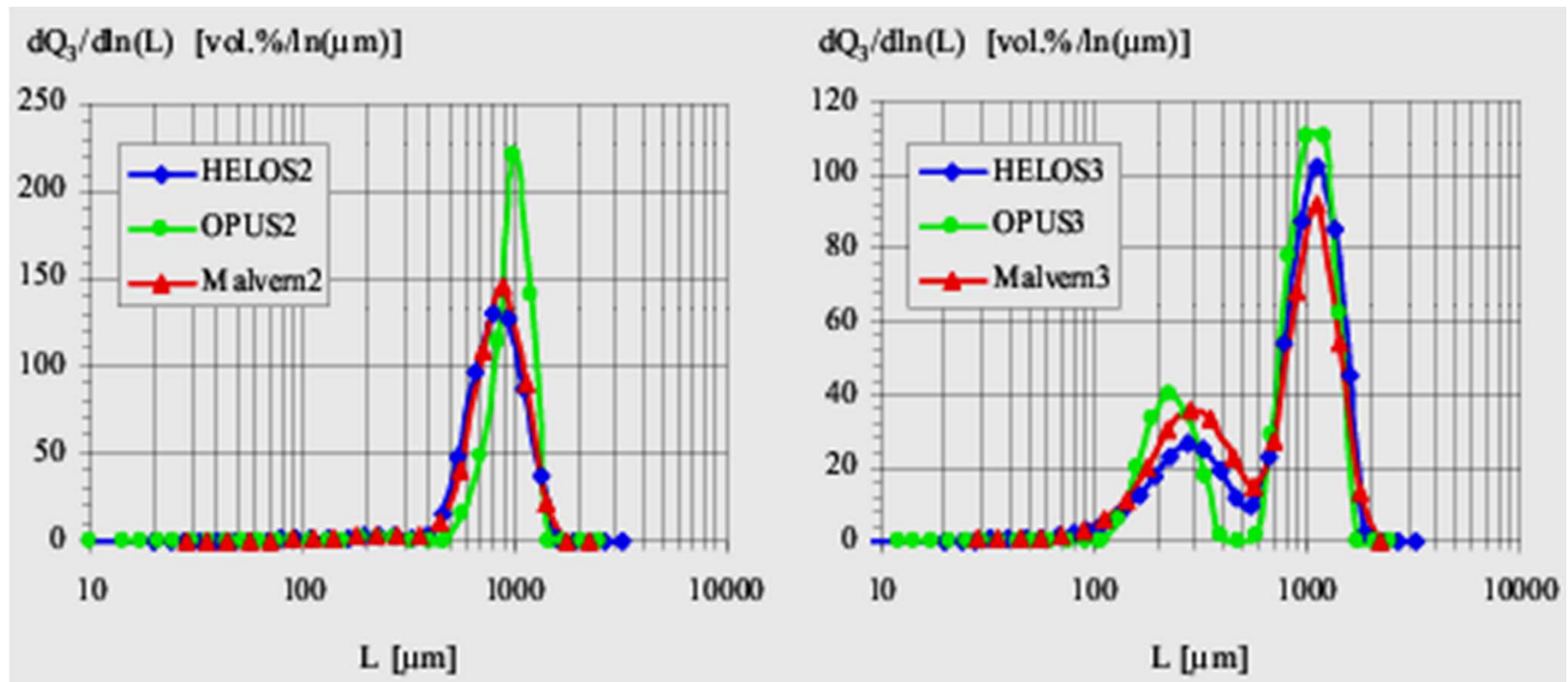
To find the size distribution $f(L)$ a suitable deconvolution technique should be adopted.

Comparison between ultrasonic attenuation and FLS*

Helos (FLS by Sympatec), Malvern2 (FLS),
OPUS (UA by Sympatec).

Ultrasonic

FLS



Ultrasonic attenuation - Conclusions

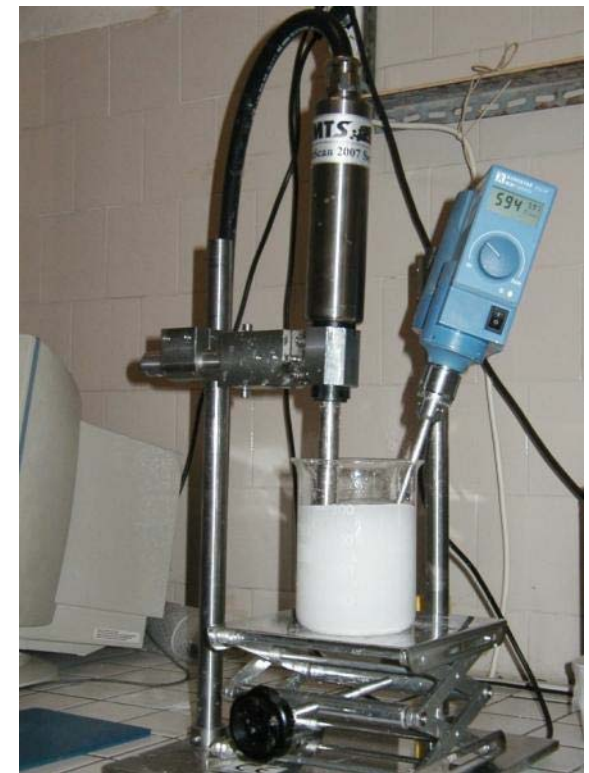
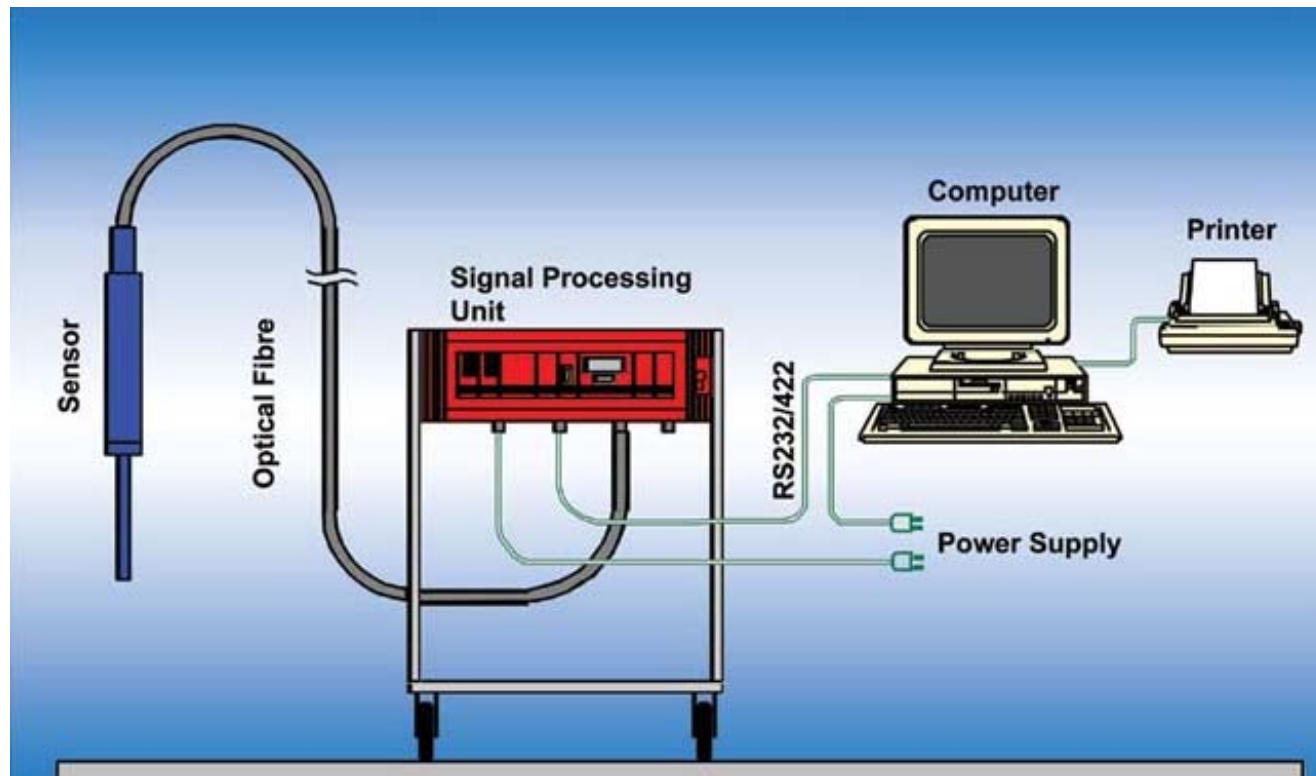
- Mass based volume distribution
- Suitable for on-line measurement
- Volume concentration up to 70 %
- Size range: 0.1 – 3000 microns
- Information about physical properties of particles are needed for calibration, which is quite troublesome.

In-situ Sensors

- Kind of sensors
 - Light back scattering probe
 - Particle image analyser
- Sensor makers
 - Mettler Toledo-Lasentec
 - MTS

The in-situ back scattering probe (BSP) instrument used at Rome Univ.

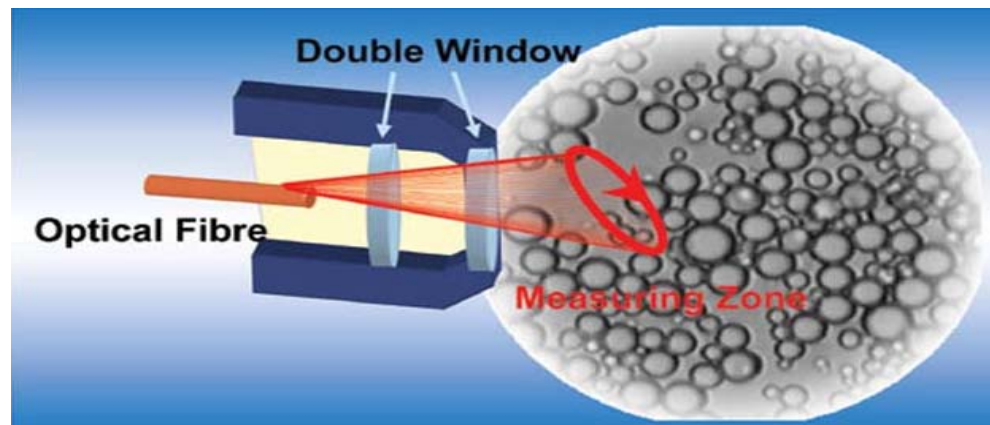
Labscan by MTS



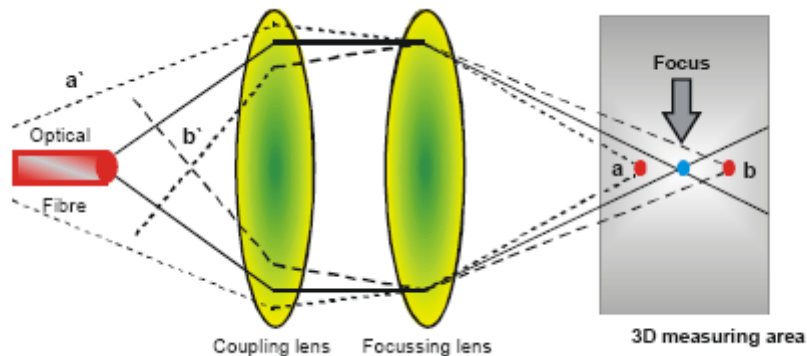
In-situ back scattering probe instrument by MTS

An infrared laser beam scans across the suspended particles

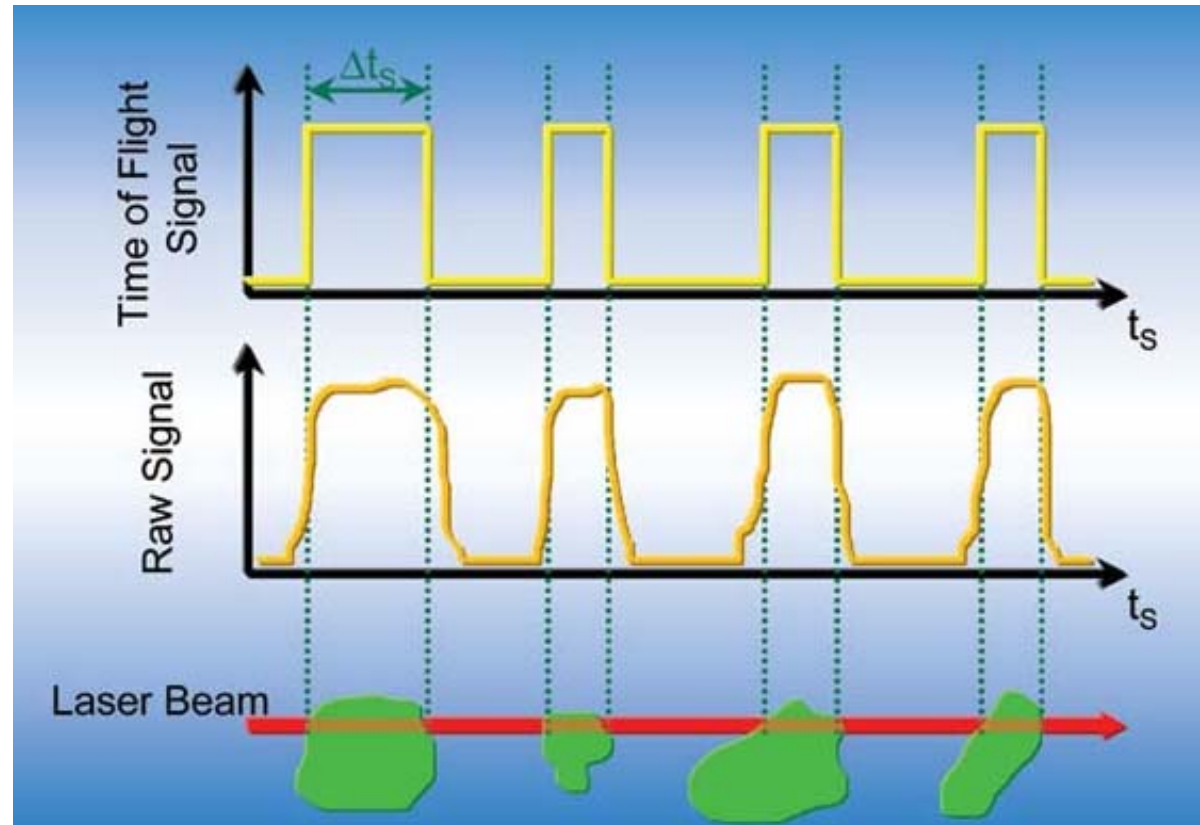
LABSCAN



MTS



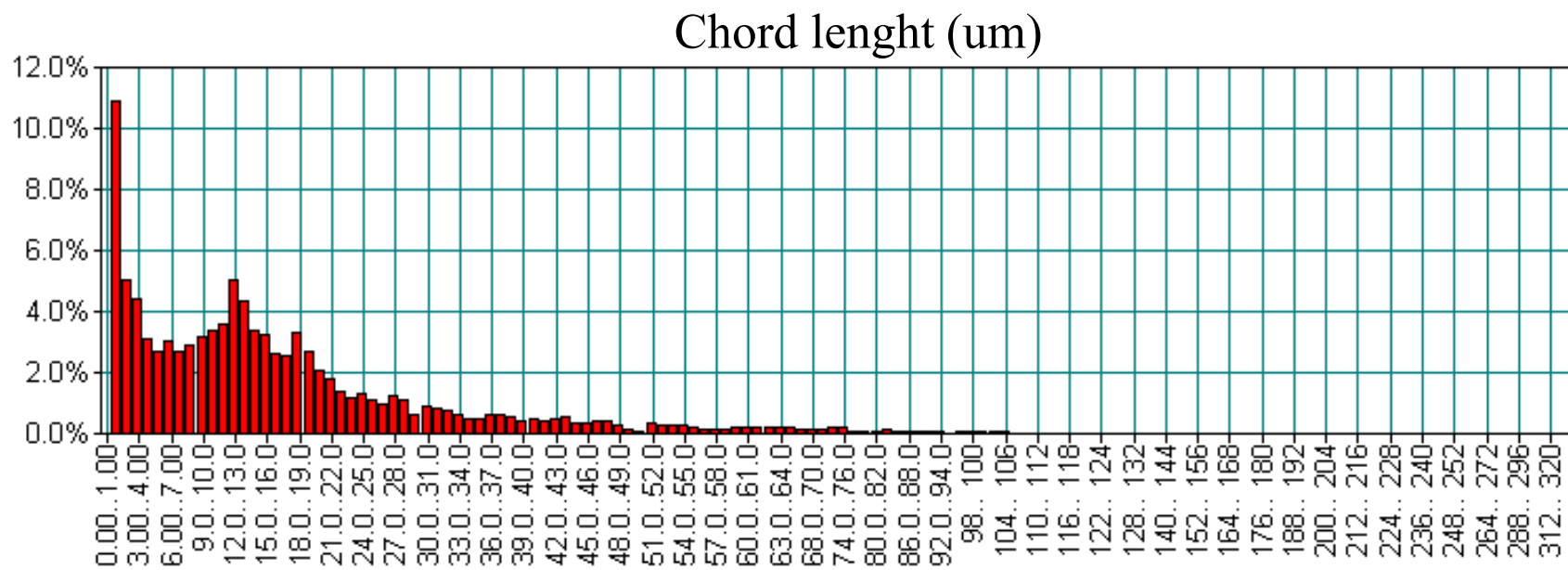
The achieved signals



The measurement is in terms of **chord length** equal to the scattered pulse duration \times the velocity of scanning

BSP instrument characteristics

- Measurement range: 0.1 – 2400 microns.
- Good reproducibility.
- Suitable for on-line monitoring and control.
- Chord lengths are measured, thus CSD must be inferred from CLD.



The correlation function between CLD and CSD

FREDHOLM Integral Equation

$$h_o(lc) = \int_{l_{c,\max}=lc}^{l_{c,\max}} p(l_c, l_{c,\max}) q_o(l_{c,\max}) dl_{c,\max}$$

h_o number distribution of chord lengths

q_o number distribution of the particles as function of size

p probability of measuring a chord length l_c when scanning a particle size $l_{c,\max}$

How to obtain CSD from CLD

- by the method of solution of Chahine, Wicksell, etc.
- by deconvolution methods

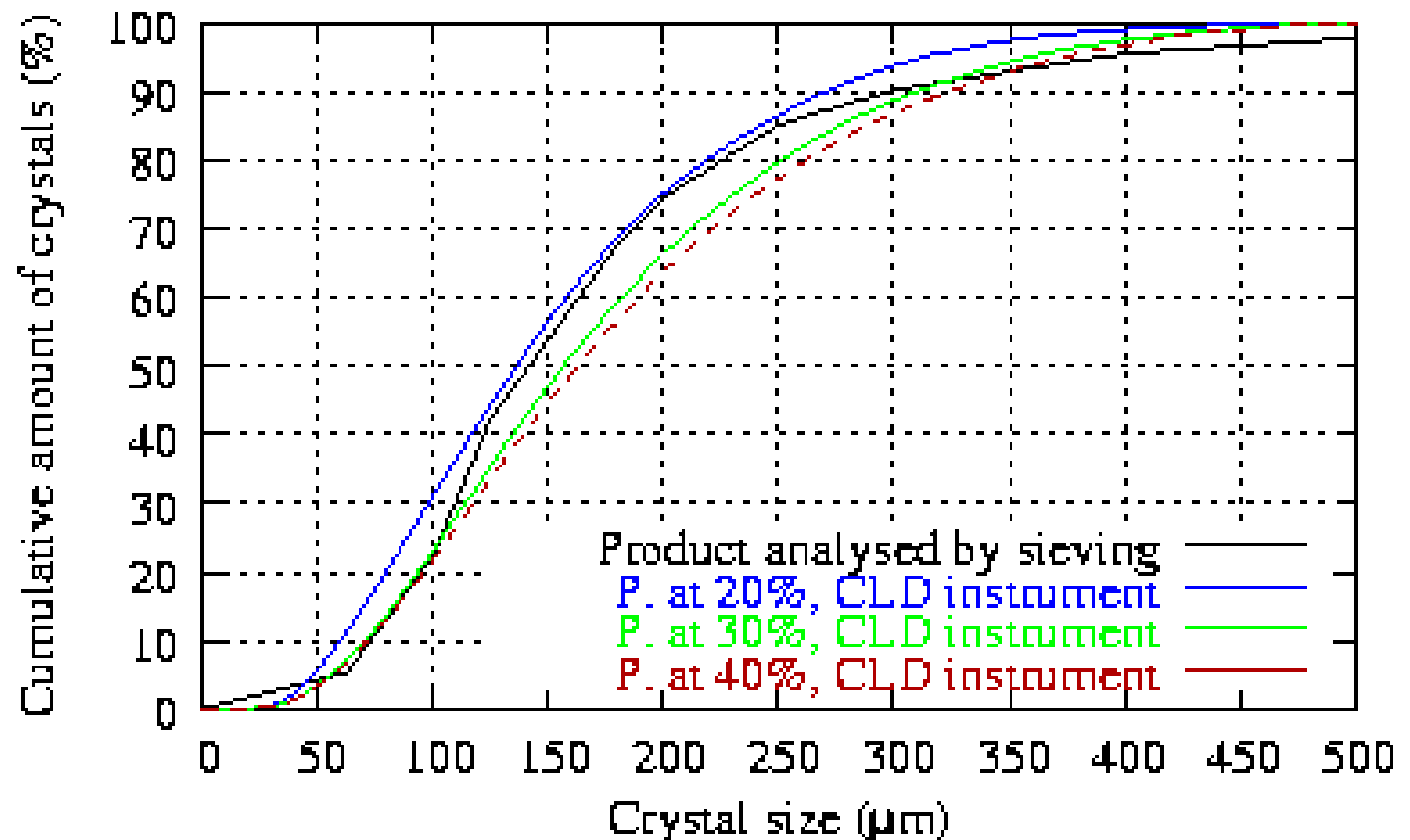
A unique relationship is not possible if both the size and shape of the particles vary

Comparison between in-situ back scattering probe and traditional sensors

- In the framework of the European project Sinc-Pro, the feasibility of using the in-situ BSP supplied by MTS (PsyA) for control purposes is studied. Comparisons have been made with:
 - sieving
 - FLS sensor

Comparison with sieving

Examined system: dextrose monohydrate

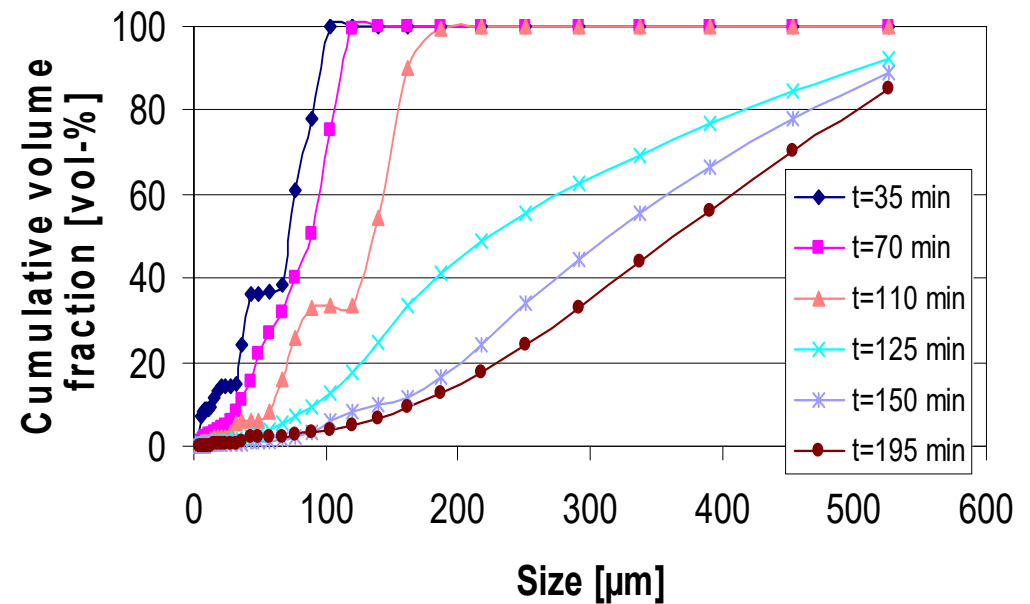
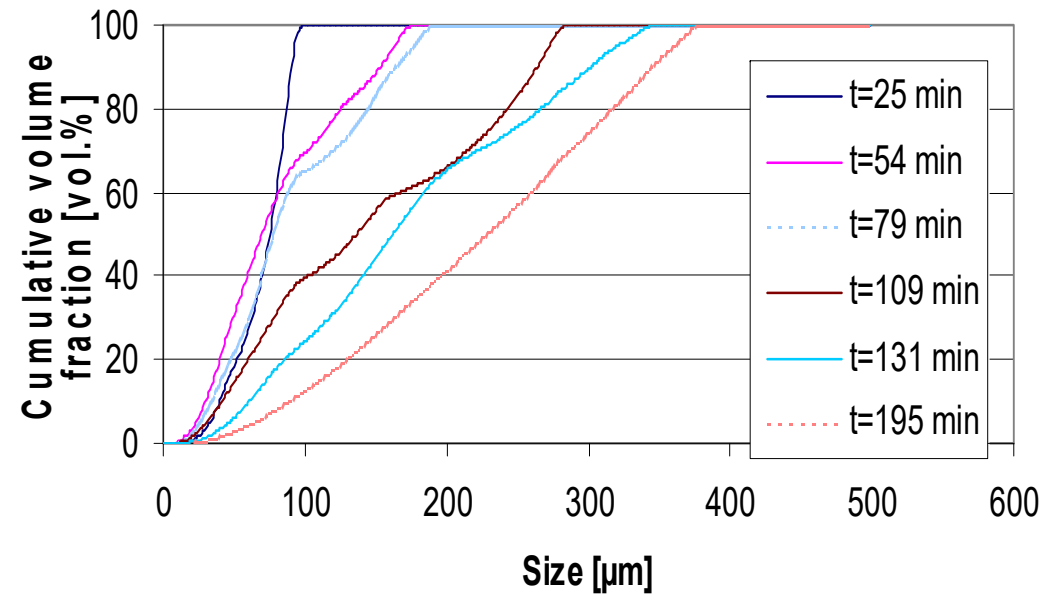


BSP

Comparison with FLS

Case study:
Crystals from a batch
crystallization

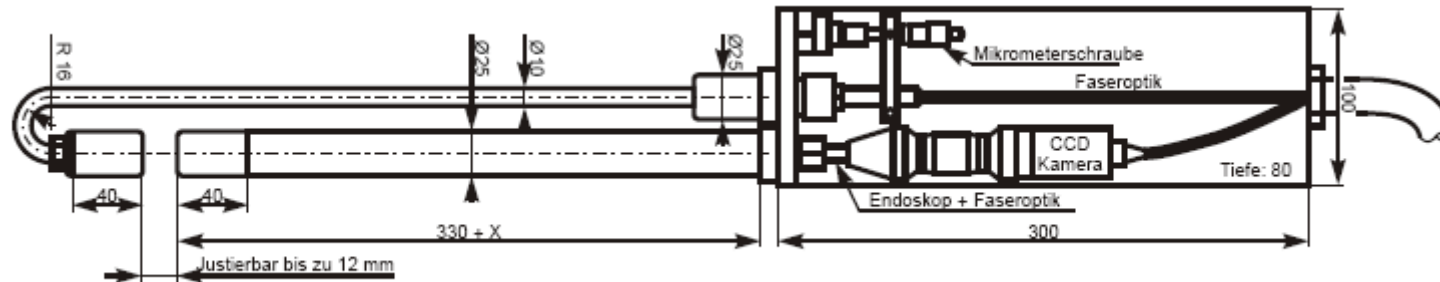
FLS



BSP instrument: Conclusions

- The slurry magma density affects the CLD.
- The resolution of the FLS is higher than that one of the in-situ BSP.
- The trend of the CSDs may be observed by means of the in-situ BSP
- Kinetic studies are hardly performed.

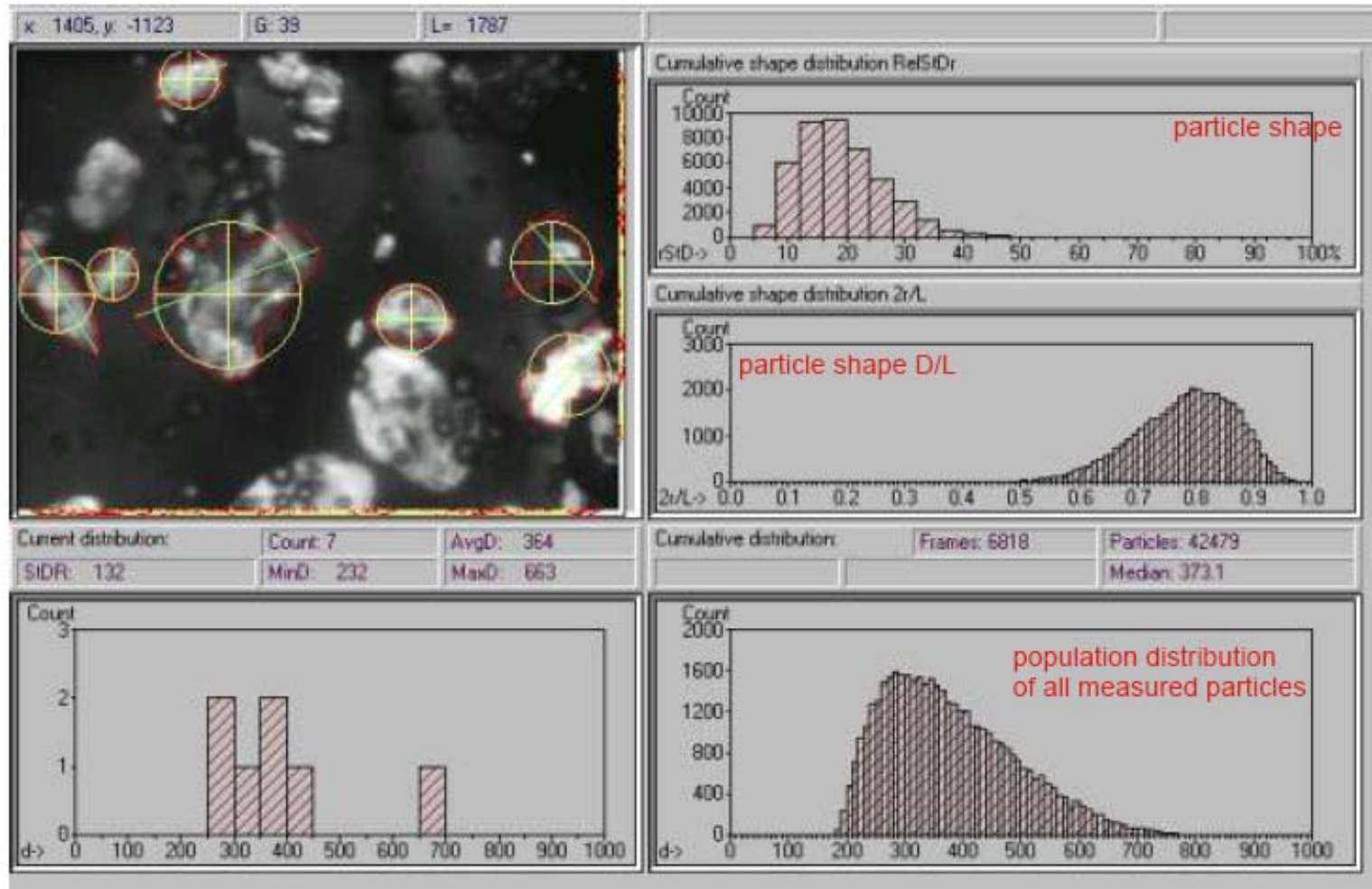
In-Process Particle Image Analysis



The on light and back
light combined method
provides fast
measurements



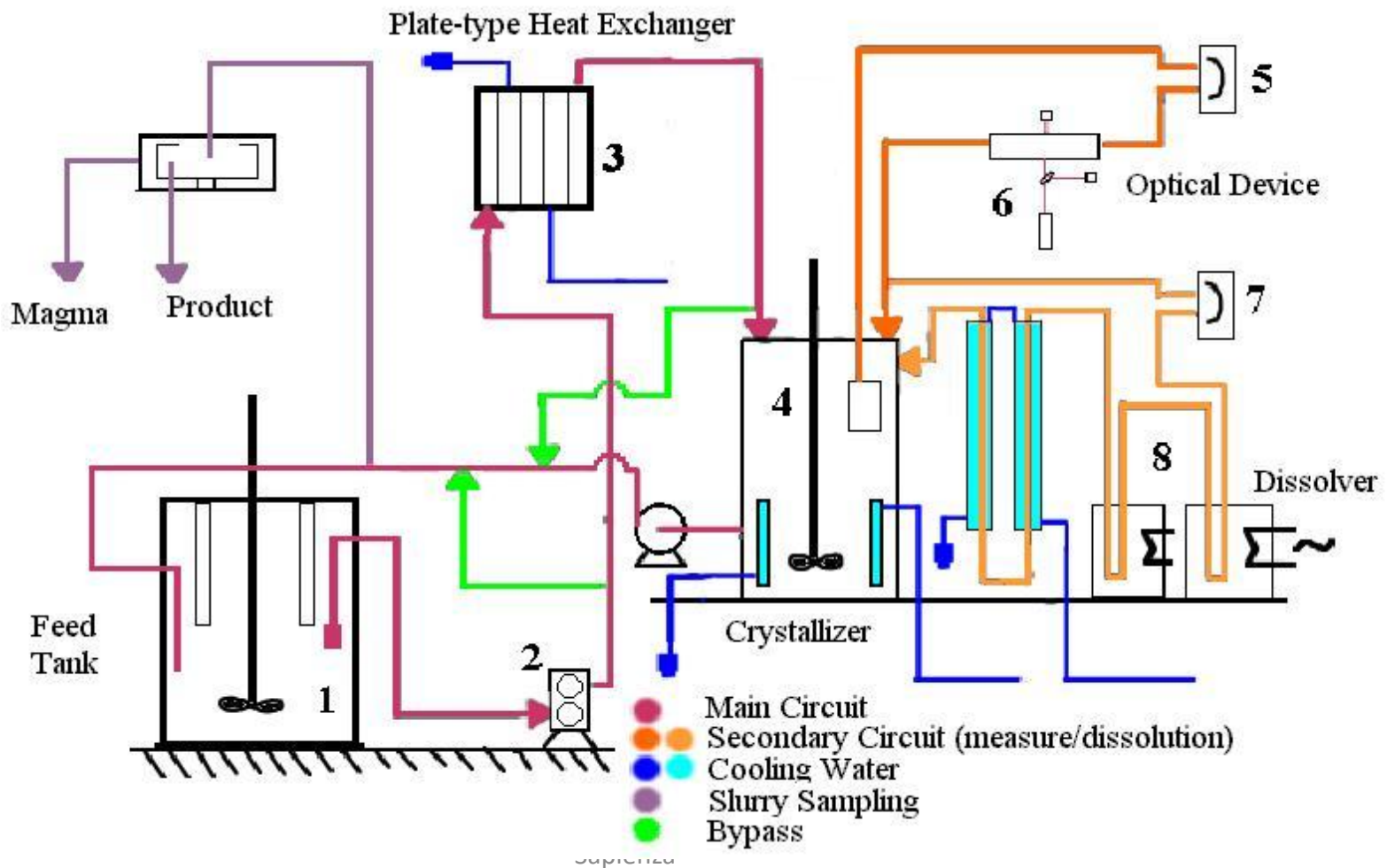
Image analysis



Considerations on in-situ image analysis instruments

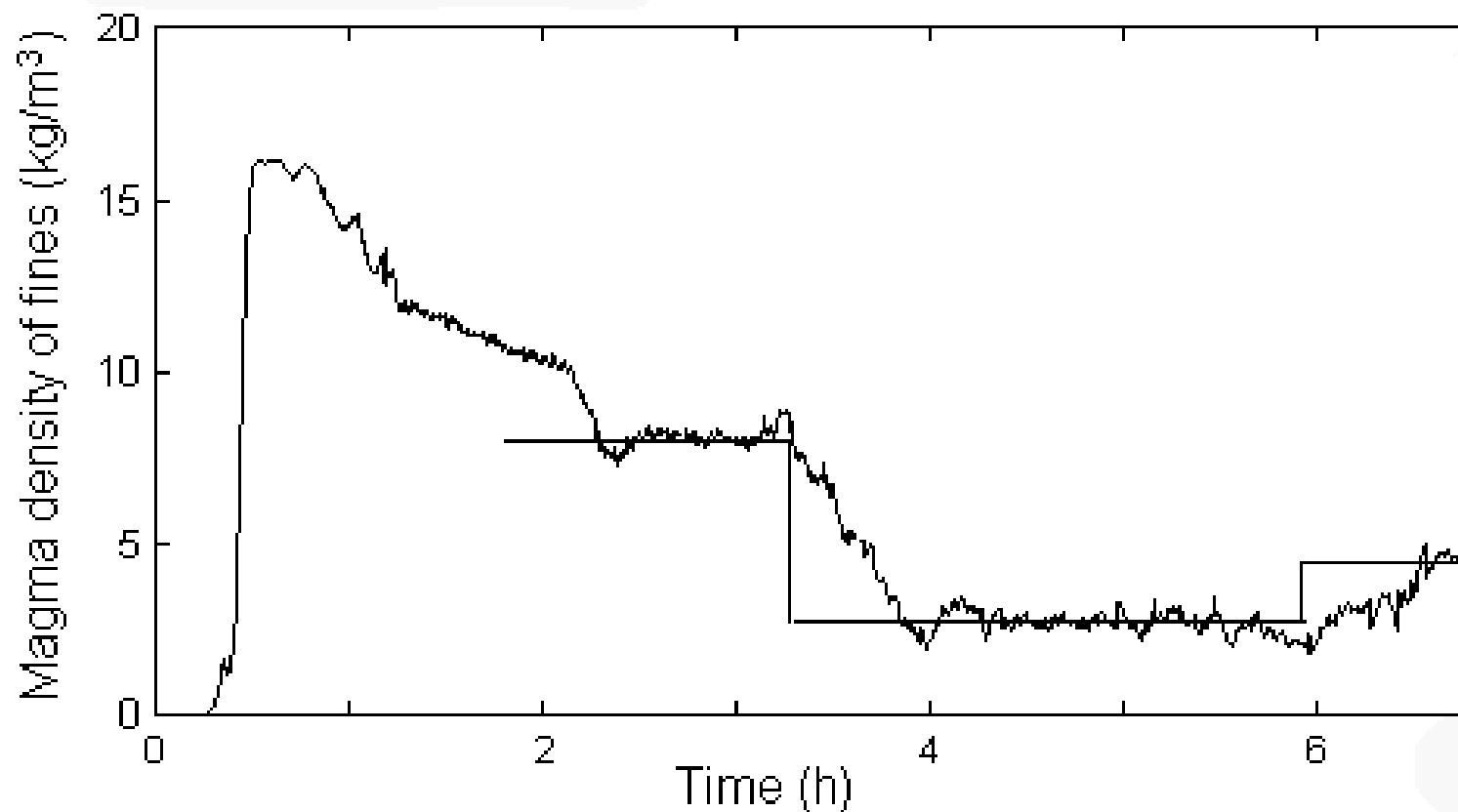
- Very suitable to monitor the crystal habit and the evolution of crystal size
- Troublesome measurement of the CSD may be obtained for high slurry magma density.
- High cost

Application of Fines meter-Plant for control purposes



Measured of $M_{T,fines}$ vs. time

Case study: Continuous Crystallization of Potassium sulphate



Fines meter sensors - Conclusions

It seems to a very suitable instrument for measuring the magma density of fines on the basis of:

- a constancy of size distribution of fines
- a calibration curve performed on the slurry to be measured

Conclusions

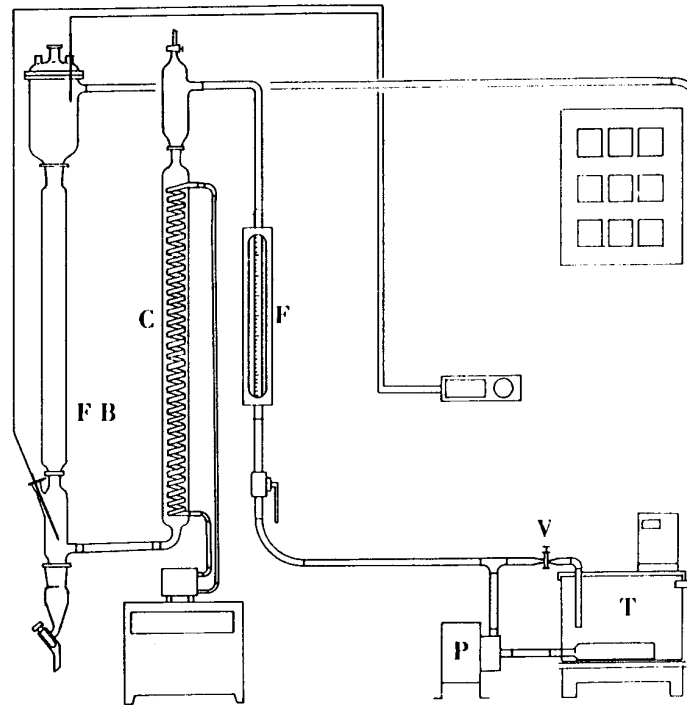
- In-situ back-scattering sensors may be used for a qualitatively monitoring.
- Ultrasonic attenuation seems to be the most suitable on-line sensor. It gives realistic CSDs.
- When the control variable is the magma density of fines, the Fines meter is a promising sensor to supervise both batch and continuous crystallization processes.

MEASUREMENT OF CRYSTAL GROWTH RATE

- The crystal growth rate measurement techniques may be distinguished in two classes refer to the conditions of constancy of super-saturation and crystals size, during each experimental run, or their progressive variation. These two cases correspond to the differential and integral techniques respectively.
- The differential technique is usually applied by using a fluidised bed crystallizer as experimental set up, whereas the integral approach makes use of whichever crystallizer.
- To obtain accurate kinetic data the differential technique is much better.

GROWTH RATE MEASUREMENT BY FLUIDIZED BED

- Solute concentration and temperature are constant and the crystal mass slightly changes (+ 20-30 %) throughout each run.



- As soon as the process is stable a few grams of seed crystals, ranged in a narrow size, are gently poured into the growth zone through a tube.
- At the end of each run the flow circulation is stopped and the crystals are discharged by means of a bottom valve.

DETERMINATION OF CRYSTAL GROWTH RATE FROM DIFFERENTIAL GROWTH EXPERIMENTS

From the obtained results

- The linear growth rate can be determined as follows:

$$G = \frac{M_{fin}^{1/3} - M_{in}^{1/3}}{(\alpha \rho_c N_c)^{1/3} t}$$

- The growth rate in mass can be determined by referring the precipitated mass, ΔM , to the average crystal surface, A_{av} , that is:

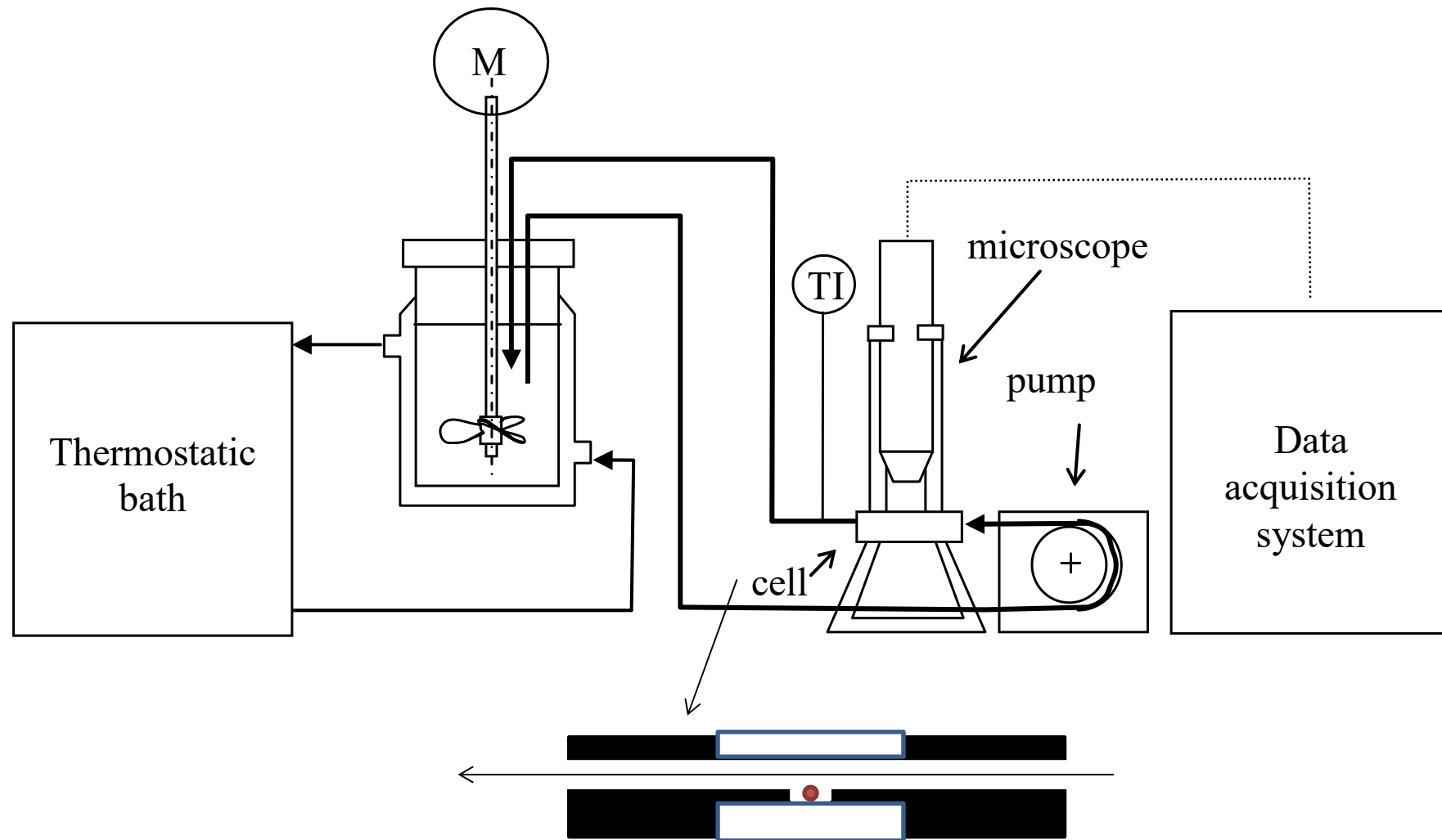
$$R_G = \frac{\Delta M}{A_{av} \cdot t}$$

- The average crystal surface can be evaluated from the initial and final CSDs

$$A_{av} = \frac{k_s}{2k_v \rho_c} \left(\frac{M_{in}}{L_{av,in}} + \frac{M_{fin}}{L_{av,fin}} \right)$$

The Experimental Apparatus

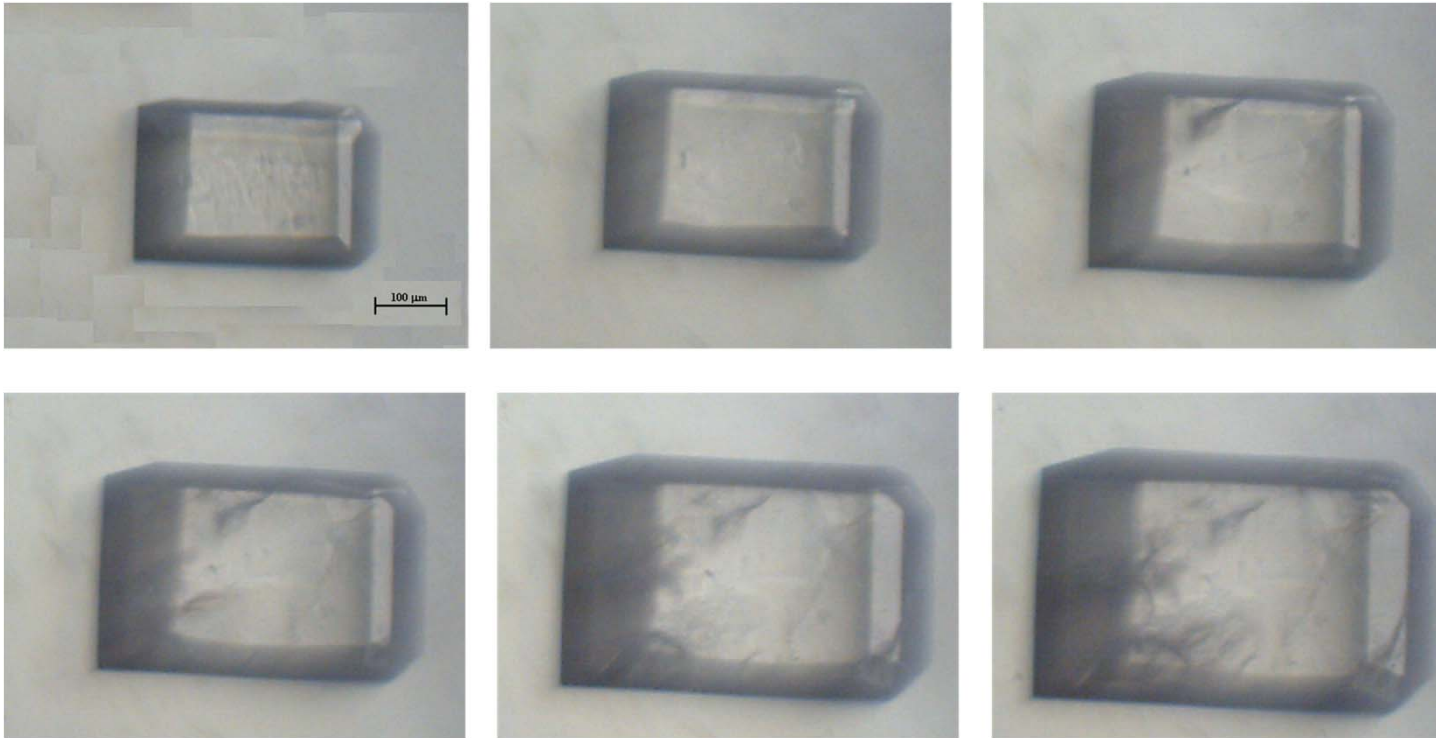
Measurement of a single crystal growth



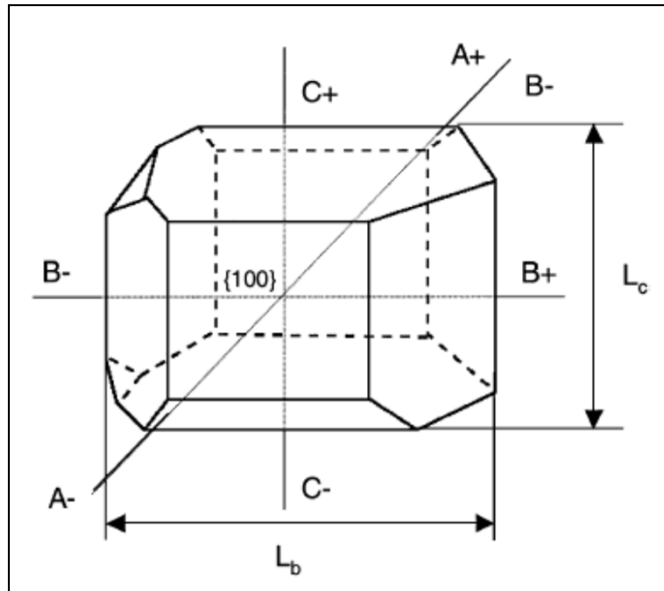
The Experimental Procedure

- A sucrose solution was prepared several hours before the run, homogenized at high temperature and then cooled down to reach the required supersaturation.
- one or two crystals are placed in the cell.
- The supersaturated solution is pumped across the cell at a low rate, about 50 ml/min, to avoid any crystal displacement.
- The temperature of the cell inlet stream was continuously monitored by a digital thermometer with an accuracy of ± 0.1 °C.
- The images were acquired at fixed intervals of time ranging between 10 and 30 minutes.
- The crystal dimensions in the two main directions were determined by the image SW code “Image J”.

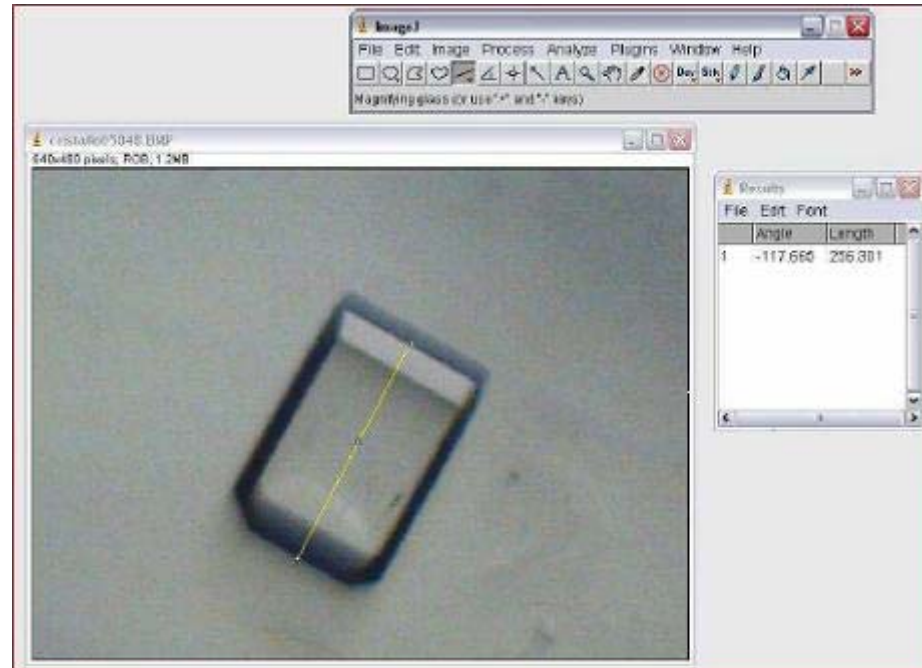
The Crystal Growing in the Cell



Characteristic dimensions

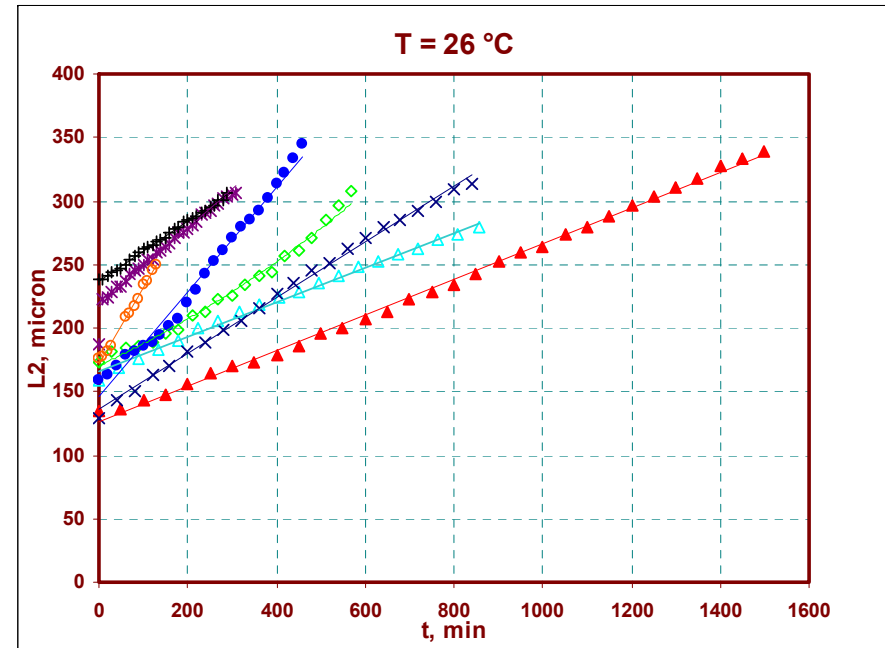
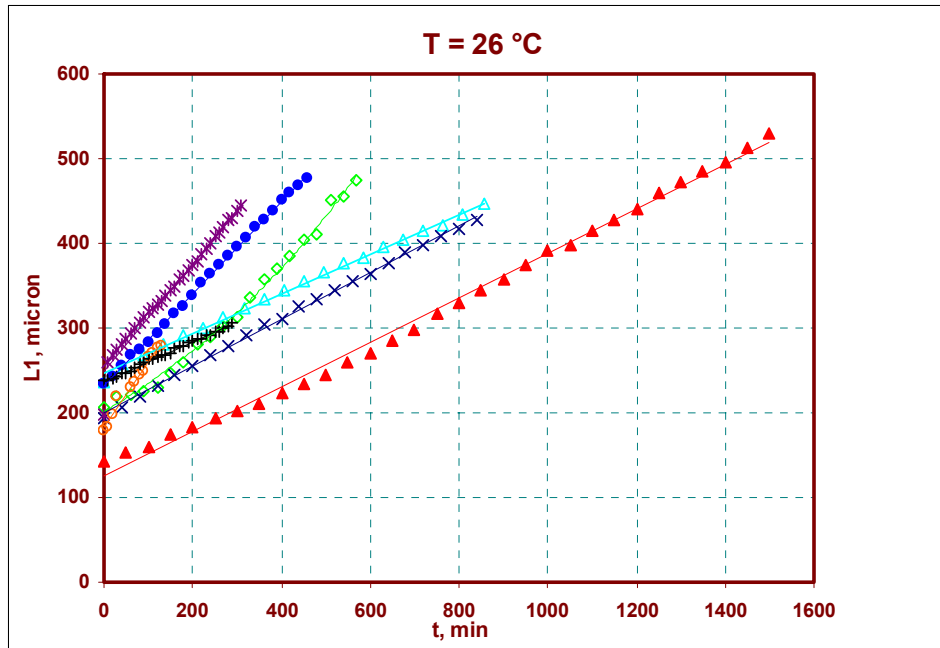


from N. Faria, M.N. Pons, S. Feyo de Azevedo, F.A. Rocha, H. Vivier, Quantification of the morphology of sucrose crystals by image analysis, Powder Technology 133 (2003) 54–67.



Screenshot from the SW ImageJ during the crystal dimensions measuring.

Growth Rate Dispersion

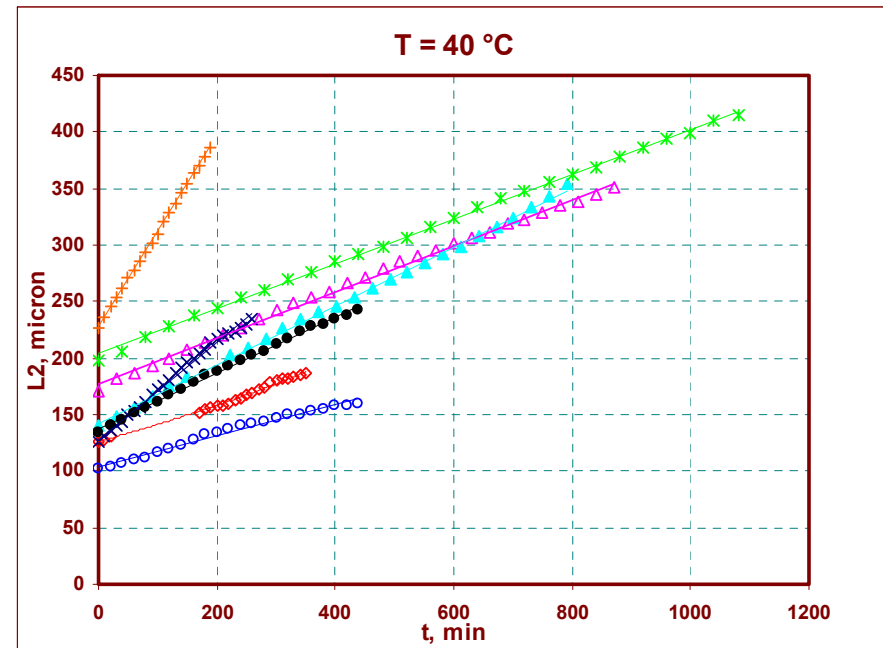
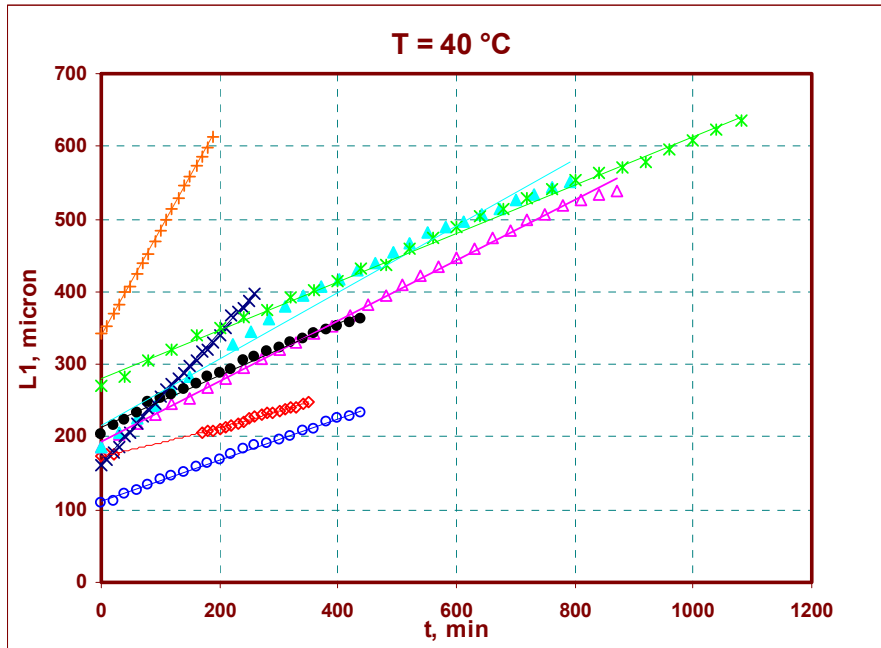


Growth Rate Dispersion

Run at 26°C and 10% of relative supersaturation (sucrose concentration: 70.1% b.w.).

RUN	$L_1 (t=0)$	G_1	R	$L_2 (t=0)$	G_2	R	G_1/G_2
ID	μm	$\mu\text{m}/\text{min}$	#	μm	$\mu\text{m}/\text{min}$	#	#
1A	206	0.49	0.991	173	0.23	0.987	2.2
1B	236	0.23	0.998	159	0.14	0.997	1.7
1C	143	0.26	0.998	134	0.14	0.999	1.9
1D	194	0.28	0.999	130	0.22	0.999	1.3
1E	198	0.54	0.999	187	0.41	0.993	1.3
1F	235	0.63	0.986	159	0.31	0.981	2.1
1G	178	0.78	0.990	176	0.60	0.996	1.3
1H	238	0.23	0.998	180	0.23	0.999	1.0
mean		0.43			0.28		1.6
st. dev.		0.21			0.16		0.4

Growth Rate Dispersion



Growth Rate Dispersion

Run at 40°C and 10% of relative supersaturation (sucrose concentration: 72.4 % b.w.).

RUN	$L_1 (t=0)$	G_1	R	$L_2 (t=0)$	G_2	R	G_1/G_2
ID	μm	$\mu\text{m}/\text{min}$	#	μm	$\mu\text{m}/\text{min}$	#	#
2A	174	0.21	0.996	126	0.18	0.993	1.2
2B	186	0.42	0.999	171	0.20	0.999	2.0
2C	186	0.46	0.989	141	0.26	0.999	1.8
2D	162	0.90	0.999	126	0.43	0.997	2.1
2E	270	0.33	0.999	198	0.20	0.999	1.7
2F	203	0.36	0.996	135	0.25	0.998	1.4
2G	108	0.29	0.999	102	0.14	0.992	2.1
2H	342	1.45	0.999	227	0.84	0.999	1.7
mean		0.55			0.31		1.8
st. dev.		0.42			0.23		0.3

Growth Rate Dispersion

It appears evident that, at both examined temperatures, the growth rate values are highly scattered. Moreover, also the ratio of the growth rates along the first and the second dimension considerably changes from crystal to crystal, as shown in the tables.

These variations in the growth rate along both the main axes of the crystals can be explained by the well-known phenomenon of growth rate dispersion, which reflects the presence of different numbers of dislocation step sources at the surface of the growing crystals.

Therefore the technique may be used to check the relationship between crystal growth and concentration, temperature, etc. only by using and analyzing the same crystal.

Growth Rate Dispersion

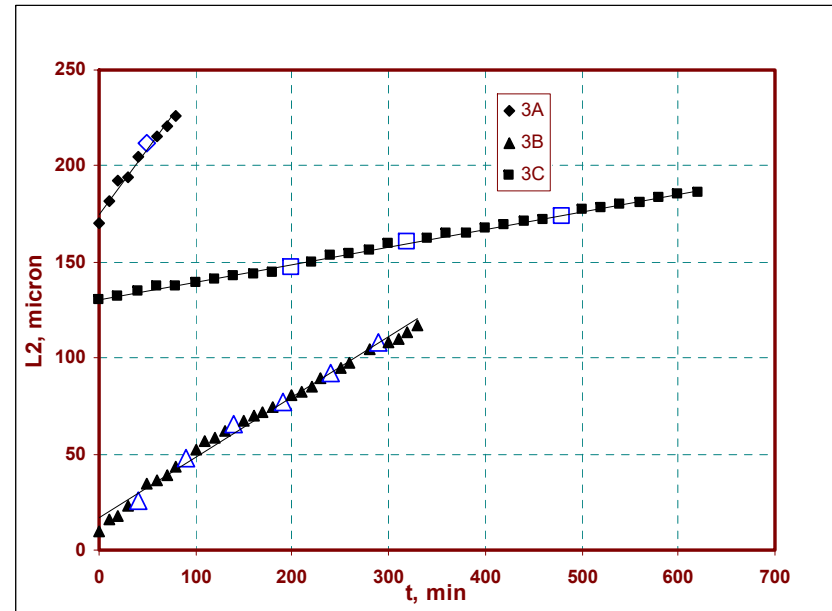
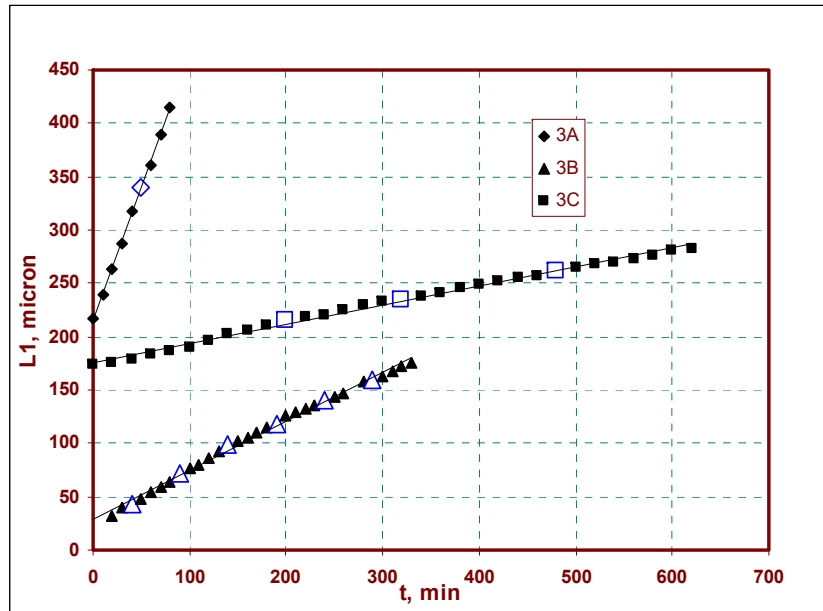
The calculated value of the mean growth rates are comparable with the one reported in the literature: for instance, at 30°C for a 10% relative supersaturation, a linear growth rate of 0.5 $\mu\text{m}/\text{min}$ is reported in P. Honig: Principle of sugar technology, Elsevier, Amsterdam, 1953.

The growth rate dispersion among crystals is quite high, thus each effect must be evaluated by the change in the operating condition applied to the same crystal.

The Temperature Effect

RUN	w	cooling policy		G ₁	R	G ₂	R	G ₁ /G ₂
ID	% <u>b.w.</u>	Δt (min)	T (°C)	$\mu\text{m}/\text{min}$	#	$\mu\text{m}/\text{min}$	#	
3A	72.4	50	40	2.48	0.999	0.67	0.988	3.7
		30	35					
3B	72.4	40	40	0.46	0.997	0.31	0.995	1.5
		50	35					
		50	30					
		50	25					
		50	20					
		50	15					
		40	10					
3C	70.1	200	26	0.18	0.997	0.09	0.999	1.9
		120	21					
		160	16					
		140	11					

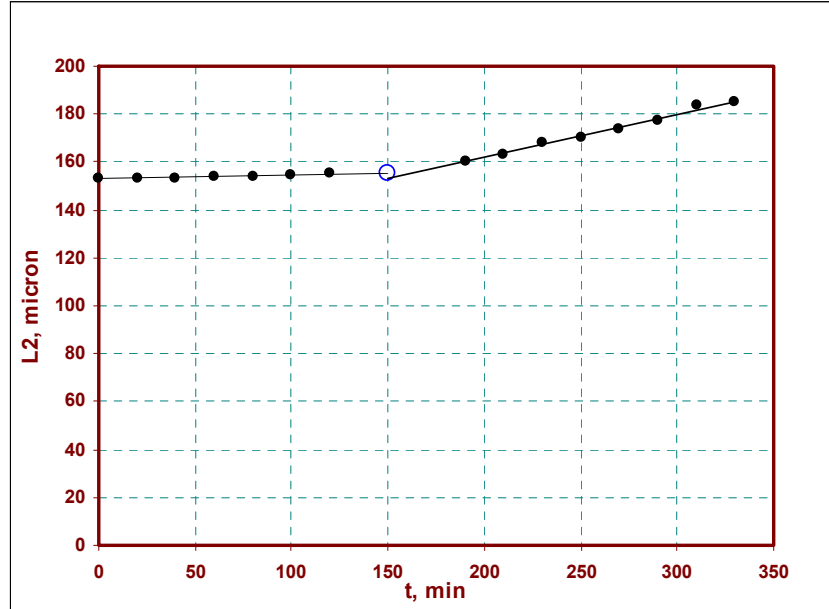
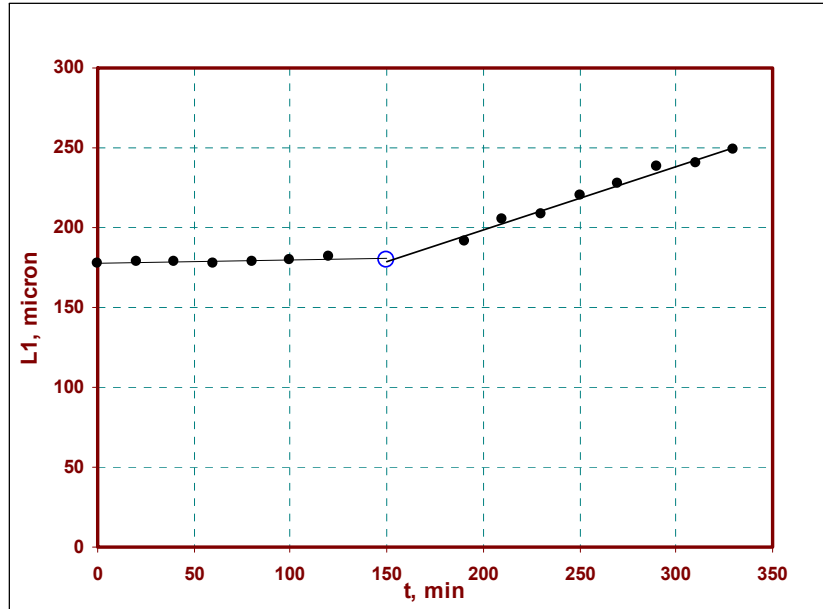
The Effect of Temperature



At the blue dots, temperature changes (reduction) were performed.

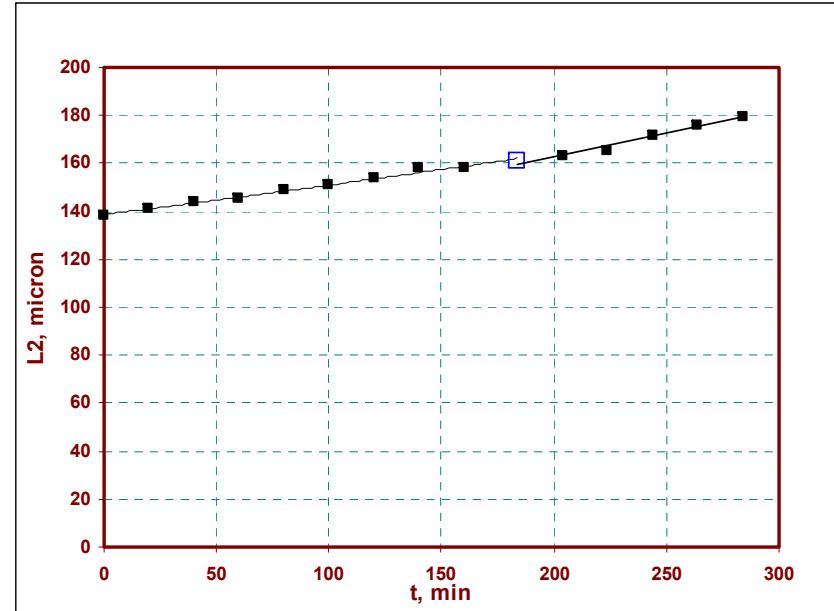
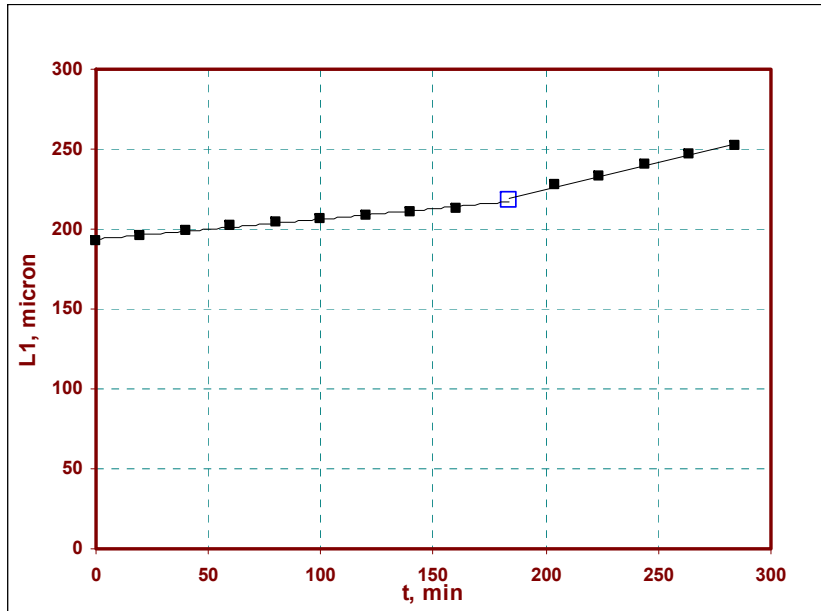
The effect is negligible, probably kinetics and thermodynamic effects are counterbalanced.

The Concentration Effect



At the blue dot, concentration was increased at fixed temperature.

The Effect of Concentration



Again, the effect is clearly detectable: the concentration increase correspond to a growth rate increase. Nevertheless, for a quantitative evaluation, more data are needed.

At a supersaturation equal to 20% nucleation may take place.

Nucleation in the cell

